https://doi.org/10.5194/egusphere-2026-3072
Preprint. Discussion started: 1 July 2026

The role of climate-society impacts in an Integrated Assessment Model: feedbacks, cascades and interdependencies

Adakudlu Muralidhar[1], Cecilie Mauritzen[2], Christopher D. Wells[3], Benjamin Blanz[4], William Schoenberg[5,13], Beniamino Callegari[6], Jannes Breier[7], Jefferson K. Rajah[5], Lennart Ramme[8], Andreas Nicolaidis Lindqvist[9], Alexandre C. Köberle[10], Axel E. Eriksson[10,12], Chris Smith[11]

[1]Division for Ocean and Ice, Norwegian Meteorological Institute, Oslo, 0313, Norway
[2]Division for Climate, Norwegian Meteorological Institute, Oslo, 0313, Norway
[3]School of Earth and Environment, University of Leeds, Leeds, LS2 9JT, United Kingdom
[4]Research Unit Sustainability and Climate Risks, University of Hamburg, Grindelberg 5, 20144 Hamburg, Germany
[5]System Dynamics Group, University of Bergen, Bergen, 5020, Norway
[6]School of Economics, Innovation and Technology, Kristiania University of Applied Sciences, Oslo, Norway
[7]Department of Earth System Analysis, Potsdam Institute for Climate Impact Research, Telegrafenberg A31, 14473, Potsdam, Germany
[8]Max-Planck-Institute for Meteorology, Bundesstraße 53, 20146 Hamburg, Germany
[9]RISE Research Institutes of Sweden, Ideon Beta5, Scheelevägen 17, 22370, Lund, Sweden
[10]Instituto Dom Luiz, Faculty of Sciences, Universidade de Lisboa, Campo Grande, Edifício C1, Piso 1, 1749-016, Lisboa, Portugal
[11]Energy, Climate and Environment Program, International Institute for Applied Systems Analysis (IIASA), Laxenburg, 25 Austria
[12]Stockholm Resilience Centre, Stockholm University, Albanovägen 28, SE-106 91 Stockholm
[13]isee systems inc., 24 Hanover St, Ste 8A, Lebanon, NH 03766 USA

Correspondence to: Cecilie Mauritzen (ceciliem@met.no)

Abstract. Conventional Integrated Assessment Models (IAMs), including those used in Shared Socioeconomic Pathway (SSP) projections, often represent climate damages with limited cross-sectoral coupling, potentially missing system–wide and nonlinear risks. Policy approaches that assume gradual, reversible, and predictable change are therefore likely to underestimate both the risks of delayed action and the benefits of early, coordinated intervention. These limitations highlight the need for IAMs to incorporate increasingly comprehensive representations of climate–society feedbacks in order to better characterize climate risks under real-world conditions.

To address this gap, this study investigates how explicit climate–society feedbacks alter long-term projections in a coupled human–Earth system. We use the Feedback-based knowledge Repository for Integrated Assessments version 2.1 (FRIDA v2.1), a global IAM designed to capture bidirectional feedbacks between climate and multiple socio-economic modules—Energy, Finance, Demography, Human Behaviour, Land Use, and Resource Infrastructure—via 19 climate impact channels grouped into 9 broader categories.

We compare a counterfactual simulation ensemble without climate-society impacts (NoImpacts) to a fully coupled experiment with all the impact channels (AllImpacts), and to experiments where impact channels are activated individually. Across these experiments, we find that explicit climate feedbacks fundamentally alter socioeconomic trajectories, with the

https://doi.org/10.5194/egusphere-2026-3072
Preprint. Discussion started: 1 July 2026

AllImpacts case exhibiting substantially lower economic growth than the NoImpacts case due to cascading feedback loops that propagate through financial, energy, demographic, and resource systems. Indirect economic channels—particularly climate-induced changes in investment and bank assets—emerge as the dominant drivers of system-wide outcomes, while other impacts remain largely sector-specific. These cascading mechanisms imply a growth-damage rather than a level-damage representation of climate impacts relative to canonical IAMs (e.g., DICE), resulting in substantially larger economic losses.

The analysis reveals strongly nonlinear climate-society interactions driven by cross-sectoral feedbacks, state-dependent responses, and regime-switching dynamics. Nonlinearities are particularly pronounced in food demand, crop yield, agricultural water use, and surface temperature anomaly, reflecting heterogeneous response mechanisms across coupled biophysical and socio-economic systems. These results demonstrate that tightly coupled human-Earth systems can generate non-linear system-wide changes even in the absence of explicit tipping elements.

1 Introduction

Climate change poses risks that emerge from interactions between the biophysical and socio-economic systems and propagate through interconnected economic and societal processes. However, much of the current modeling architecture continues to treat these domains separately. In widely used emissions scenario frameworks, such as the Shared Socioeconomic Pathways (SSPs; Riahi et al., 2017) used in Intergovernmental Panel on Climate Change Sixth Assessment Report (IPCC AR6 WGII, 2022) and within the recent Climate Model Intercomparison Project Phase 6 (CMIP6; Frieler et al., 2024), climate change is typically simulated independently from its impacts, which are evaluated using sector-specific impact models. While this separation enables methodological consistency and comparability across studies, and avoids double counting of the impacts (Moss et al., 2010; O'Neill et al., 2014), it implicitly assumes that climate impacts can be represented as downstream, which limits the understanding of the coupled feedbacks between the climate and human society. Integrated Assessment Models (IAMs) have been used to partially bridge this split by linking climate change with economic evolution. However, they generally rely on highly aggregated representations of impacts, through aggregate damage functions or loosely coupled sectoral modules (Nordhaus, 2017; Tol, 2018; Schwanitz et al. 2019; Reilly et al., 2007; Stern, 2013; IPCC AR6 WGII, 2022). These approaches offer computational tractability, consistency, transparency, and ease of calibration. At the same time, they often neglect structural interdependencies between impact channels, implicitly assuming that sectoral damages can be combined in an additive manner. This simplification may obscure the ways in which climate impacts propagate across sectors and interact through shared economic and biophysical processes.

A growing body of literature suggests that neglecting such interdependencies can bias estimates of climate risk. Bressler (2021) shows that conventional IAMs often omit or underrepresent key impact channels, such as temperature-related mortality, leading to potential underestimation of damages. Limited representation of interactions between impact channels may lead to both under- and over-estimation of the actual damages, particularly when nonlinear feedbacks generate

https://doi.org/10.5194/egusphere-2026-3072
Preprint. Discussion started: 1 July 2026

reinforcing or offsetting effects across channels (Burke et al., 2015; Dietz et al., 2021; Howard and Sterner, 2017). In addition, recent work highlights the potential for cascading and systemic risks, including implications for financial stability and macroeconomic performance (Battiston et al., 2017; Bolton and Kacperczyk, 2020). Extending this perspective, network-based analyses of the climate–economy nexus show that endogenous feedbacks within interconnected financial systems can amplify and propagate climate-induced shocks in nonlinear ways, suggesting that models which abstract from such network structures may understate systemic risk and mischaracterise its distribution (Battiston et al., 2017; Roncoroni et al., 2021). These findings underscore the need for modelling frameworks that explicitly represent cross-sector interactions and treat multiple impact channels with comparable structural importance, rather than implicitly prioritizing some sectors over others.

At the same time, sectoral impact models have advanced significantly, providing detailed representations of climate effects on systems such as agriculture, health, energy, and ecosystems (Rosenzweig et al., 2014; Carleton et al., 2022). However, these models are typically developed and applied in isolation, limiting their ability to capture cross-sector feedbacks and system-wide dynamics. As a result, an important knowledge gap persists: despite increasing detail in individual impact assessments, there is no consistent framework for integrating these insights into a unified system that captures cross-sectoral interactions at the global scale.

We address this gap by employing the newly developed Feedback-based knowledge Repository for Integrated Assessments version 2.1 (FRIDA v2.1) IAM (Schoenberg et al., 2025a, b), designed explicitly to represent bidirectional feedbacks between climate and socio-economic systems at the global scale. In contrast to conventional IAMs, FRIDA incorporates 19 climate impact channels and endogenizes interactions between climate and socio-economic sectors spanning financial markets, energy systems, demography, human behaviour, land use, and resource infrastructure (Wells et al., 2026). These impact channels are dynamically inter-linked, enabling changes in socio-economic conditions to influence emissions trajectories and thereby feed back into the climate system, indicating a more structurally coupled representation of climate-society interactions.

In this paper, we analyse system behaviour in terms of key drivers across six submodules associated with distinct climate impact categories and their interactions. We further examine cascading effects and the relative strength of individual impact channels within coupled feedback structures and identify sectors exhibiting pronounced nonlinearities and their underlying mechanisms.

Section 2 provides a brief description of the FRIDA model, characterization of the climate impact channels and associated principal feedback loops, and the approach to uncertainty estimation. The analysis is reported in three sections. Section 3 examines the individual contributions of each impact category to FRIDA's transition from a no-impacts counterfactual to a full-impacts representation trajectories in the socio-economic domain (Figure 4 a–k) and how these changes feed back to the climate system (Figure 4 l–n), respectively. Section 4 interprets these results by comparing the climate damages projected by FRIDA with those from the cost–benefit model DICE-2016R (Nordhaus, 2017, 2018). Section 5 examines nonlinear interactions among impact categories, defined as the difference between the aggregate of individual effects and their fully

https://doi.org/10.5194/egusphere-2026-3072
Preprint. Discussion started: 1 July 2026

coupled response, with all quantities expressed relative to the NoImpacts counterfactual, and discusses their implications. Final conclusions are presented in Section 6.

2 Methodology

2.1 The Model - FRIDA (v2.1)

This study employs the FRIDA IAM, version 2.1 (FRIDAv2.1), described in Schoenberg et al. (2025a). FRIDA comprises seven top-level modules representing key components of the World–Earth system: Climate, Economy, Energy, Human Behaviour, Resources, Land use and Agriculture, and Demographics (all depicted in Figure 1), alongside an externalized framework for socio-economic policy regulations. These modules are interconnected through multiple feedback loops, forming a complex endogenous structure that captures the co-evolutionary dynamics of the coupled system. The resulting system behaviour, termed Endogenous Model Behaviour (EMB; Schoenberg et al., 2025a), characterizes potential future pathways of the physical and socioeconomic system in the absence of additional future climate governance and behavioural interventions.

The EMB simulation, conducted over the period 1980–2150, calibrated and structurally validated for 1980–2023, serves as the reference for the analysis in this study. The EMB incorporates a set of climate impact channels, documented in Wells et al. (2026), that capture the linkages between climate and socioeconomic systems.

2.2 Climate impact channels included in FRIDA v2.1

Figure 1 provides a schematic representation of the global-scale climate-driven impacts on the socio-economic sectors covered in the FRIDA model. These impacts are functionally determined by one or more primary climate indicators - surface temperature anomaly, sea-level rise (SLR) and atmospheric CO_2 concentration, and are manifested across the six interdependent socio-economic modules. These climate-to-society feedbacks are indicated by the solid arrows in Figure 1 with module-specific colour codes.

Feedbacks to the economy include the impacts of rising surface temperature anomaly and sea-level on bank investments (indirect effects of damages to assets), worker productivity and government spending. In the demographic sector, the climate impacts cover the temperature-and sea-level-related mortality. The energy sector is influenced through temperature-driven changes in energy demand, stress on energy infrastructure, and variations in power plant efficiency. Impacts on human behaviour are determined by a modelled perception of climate extremes, including temperature and SLR, which adjusts the food demand based on the perceived risk. In the construction sector, elevated temperature and SLR affect the durability of concrete infrastructure. Finally, impacts on land use and agriculture are captured through temperature and atmospheric CO_2 effects on crop yield and agricultural water withdrawal.

The climate-driven impacts on socioeconomic sectors feed back into the climate system through subsequent changes in greenhouse gas (GHG) emissions, landuse changes and aerosol emissions, as indicated by the dotted arrows in Figure 1.

https://doi.org/10.5194/egusphere-2026-3072
Preprint. Discussion started: 1 July 2026

These changes alter radiative forcing, which in turn affects surface temperature anomaly and, consequently, sea-level anomaly (Wells et al., 2026; Ramme et al, 2025).

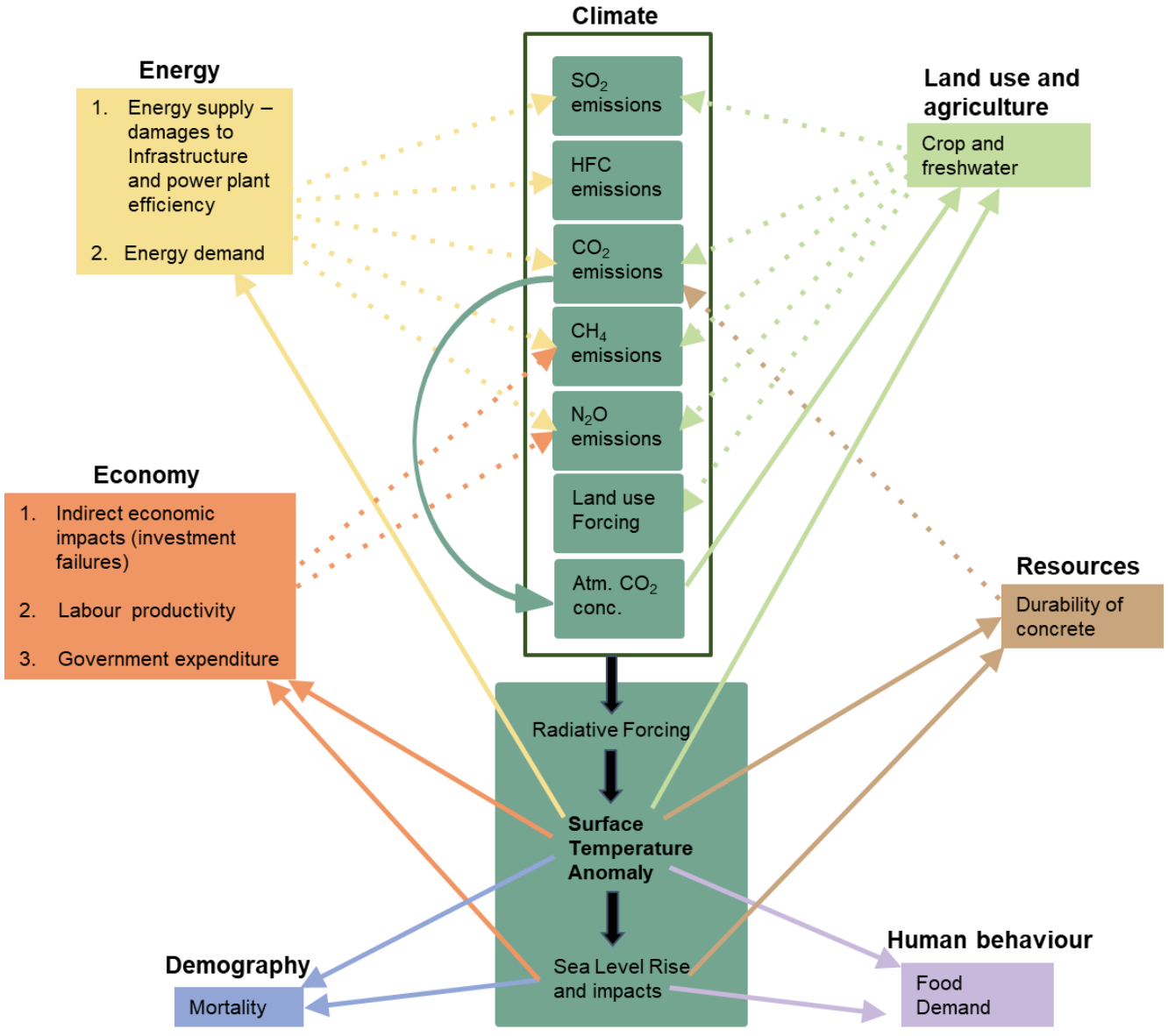

Figure 1: Overview of the global-scale linkages between the climate and the socio-economic modules in FRIDA v2.1. The modules are colour-coded to distinguish between the corresponding impact channels. Solid arrows indicate the impacts from climate to society, and dotted arrows indicate the closure of the feedbacks between the human-systems and climate through changes in the GHG emissions, landuse forcings and aerosols following the coupling structure described in FRIDA-Clim (Wells et al., 2026) and Ramme et al. (2025).

https://doi.org/10.5194/egusphere-2026-3072
Preprint. Discussion started: 1 July 2026

2.3 Principal feedback loops in FRIDA v2.1

The principal feedback loops linking the six interdependent socioeconomic modules through which the climate impacts propagate across the system, shaping the interactions among key system drivers, are shown in Figures 2 and 3. Figure 2 shows the climate impacts on economy and demography, while figure 3 covers the remaining sectors, with real GDP per capita serving as the central link across all impact pathways. In Figure 2, impacts on Economy and Demography alter real GDP per capita, driving demand for energy, food, and infrastructure, and thus influencing different emissions categories. In Figure 3, impacts on energy, infrastructure, human behaviour, and landuse affect real GDP per capita through inflation and simultaneously modulate the emissions directly via the sector-specific changes. Given the complexity of the full system, the figure is intended as a structural overview rather than a representation to be interpreted in its entirety; key feedback loops are instead examined individually in the subsections of Section 3.

The feedback loops in Figures 2 and 3 are identified through a subjective assessment of the system's response to each climate impact category individually. Table 1 summarizes the identified loops, their underlying mechanisms, and the corresponding modules. FRIDA includes many other important feedback loops that have been omitted in Figure 2 and 3 for clarity, which focus only on the subset of loops that are directly associated with the climate impact channels.

https://doi.org/10.5194/egusphere-2026-3072
Preprint. Discussion started: 1 July 2026

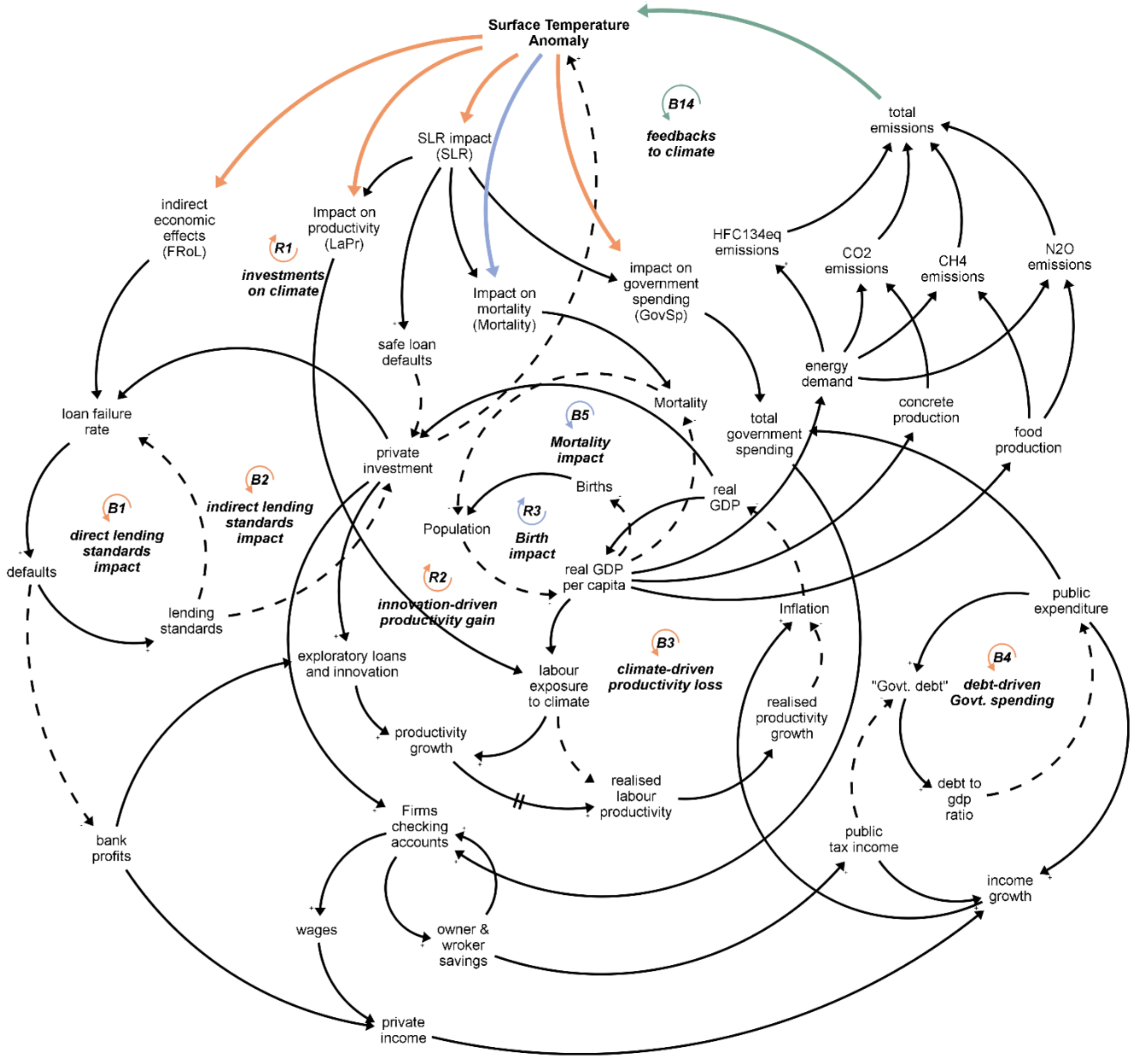

159

160 **Figure 2: Causal loop diagram highlighting key reinforcing (R) and balancing (B) feedback loops through which individual climate**
161 **impacts interact and modulate Economy and Demography. The abbreviations FRoL, GovSp, LaPr, SLR, and Mortality refer to**
162 **the experiments where the corresponding individual channels were active (see Table 2 for the list of experiments). The impacts on**
163 **Economy and Demography modify real GDP per capita, driving energy, food, and infrastructure demand. Solid (dashed) arrows**
164 **denote causal links with positive (negative) polarity.**

https://doi.org/10.5194/egusphere-2026-3072
Preprint. Discussion started: 1 July 2026

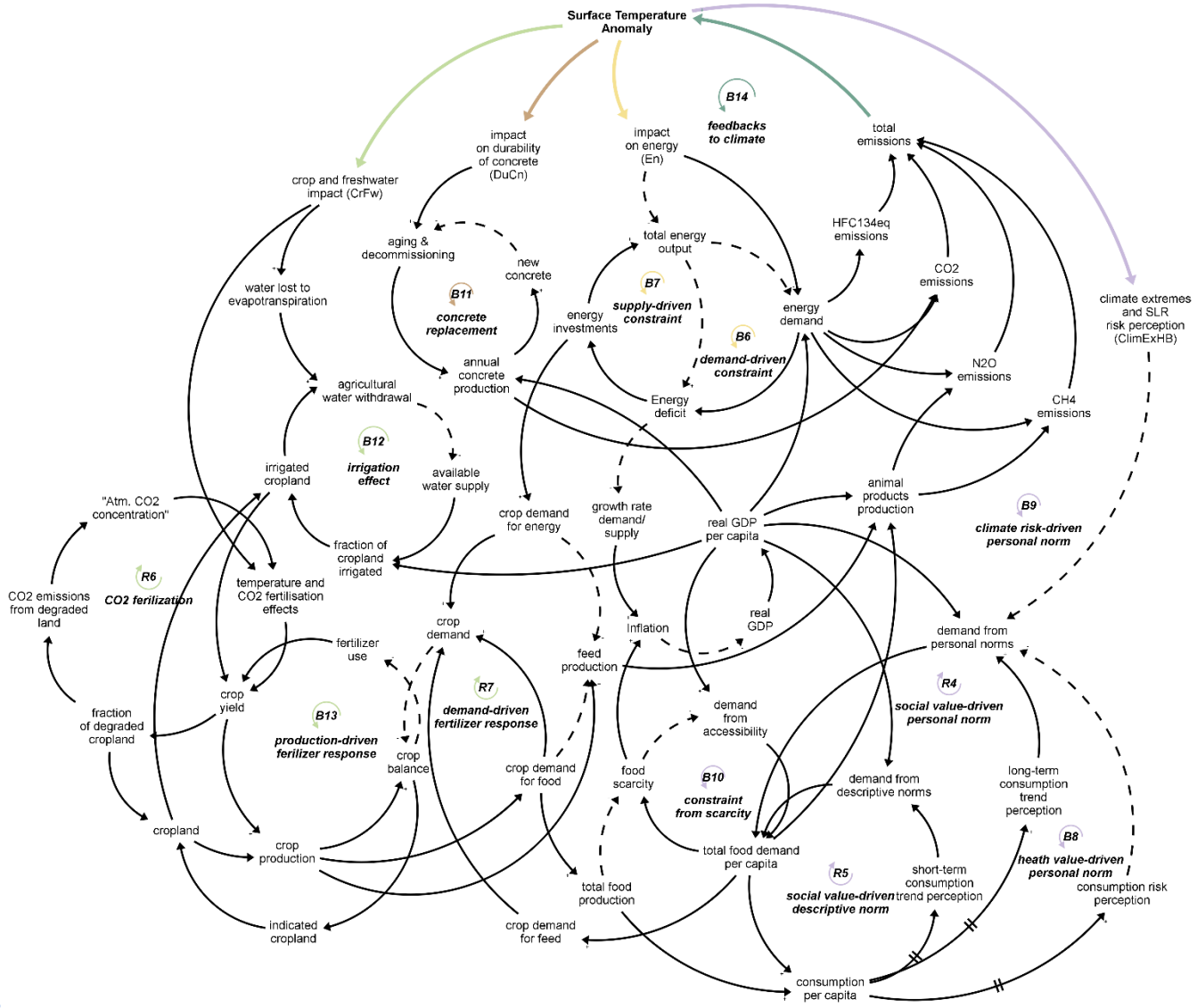

Figure 3: Same as in Figure 2, but for impacts to Energy, Human Behaviour, Infrastructure, and Land Use. Real GDP per capita is a key variable interconnecting all the impact channels. Feedback loop B14 (*feedbacks to climate*) appears in both Figure 2 and 3, representing the distinct mechanisms that influence total emissions and close the loop to the climate system (surface temperature anomaly). Solid (dashed) arrows denote causal links with positive (negative) polarity.

https://doi.org/10.5194/egusphere-2026-3072
Preprint. Discussion started: 1 July 2026

174 **Table 1: List of feedback loops from the CLD in Figure 2 and Figure 3, underlying mechanisms and associated FRIDA modules.**

Loop label	Loop name	Mechanism	FRIDA module	Link to CLD
B1	Direct lending standards impact	Tightening lending standards to improve loan quality	Economy (sec. 3.2.1)	Fig. 2
B2	Indirect lending standards impact	Reduced investment from tighter lending standards		
R1	Investments on climate	Failing of mitigation-related investments increase loan failures		
R2	Innovation-driven productivity gain	Effects of exploratory lending and innovation on productivity growth		
B3	Climate-driven productivity loss	Effects of climate exposure on labour		
B4	Debt-driven Govt. spending	Govt. taking up more debts to sustain public spending		
B5	Mortality impact	Real GDP effects on mortality	Demography (sec. 3.2.2)	
R3	Birth impact	Real GDP effects on births		
B6	demand-driven constraint	Rising demand increases energy deficit and hence investments	Energy (sec. 3.2.3)	Fig. 3
B7	supply-driven constraint	Lower supply increases energy deficit and hence investments		
B8	health value-driven personal norm	change in personal norms from perception of overconsumption	Human behaviour (sec. 3.2.4)	
R4	social value-driven personal norm	change in personal norms from long-term social value perception		
R5	social value-driven descriptive norm	change in descriptive norms from short-term social value perception		
B9	climate risk/driven personal norm	change in demand from personal norms due to climate extremes risk perception		
B10	constraint from scarcity	Food scarcity constraining the demand due to accessibility		
B11	concrete replacement	Infrastructure maintenance due to lowered concrete durability	Resources (sec. 3.2.5)	
B12	irrigation effect	Impact of water lost from evapotranspiration on irrigation efficiency	Land use and agriculture (sec. 3.2.6)	
B13	production-driven fertilizer response	fertilizer response to crop balance due to changes in crop production		
R6	CO2-fertilization	CO2 fertilization effect		
R7	demand-driven fertilizer response	fertilizer response to crop balance due to changes in crop demand		
B14	feedbacks to climate	Feedbacks to climate from the changes to radiative forcing	Whole Model	Figure 2 and 3

https://doi.org/10.5194/egusphere-2026-3072
Preprint. Discussion started: 1 July 2026

2.4 Feedback sensitivity experiments

We adopt a structural feedback sensitivity approach inspired by feedback loop dominance analysis (Ford, 1999), in which the climate–socioeconomic feedbacks are systematically enabled one at a time to assess their individual contribution to system behaviour and interactions. The experimental design in this study thus comprises a counterfactual projection without any climate impacts and a series of single-channel simulations in which only one climate impact channel is activated. An overview of these experiments is provided in Table 2.

This approach enables us to filter out feedback loops that are invariant across experiments and isolate those that actively shape model behaviour. It also facilitates the identification of nonlinear dynamics emerging from interacting feedback structures (Fiddaman, 1997; Rial et al., 2004; Meadows, 2008), including threshold behaviour, regime shifts, amplification mechanisms, and damping effects.

Table 2: List of experiments and climate impact channels associated with each experiment. In total, there are 19 in FRIDAv2.1. We experiment with 18 of those, with the combinations as shown in the table. The 19th, land carbon impact, is ON in all including the NoImpacts. This impact channel is not part of the climate-society set of channels as it is internal to FRIDA's carbon cycle, hence excluded in the experiment set-up.

Experiment name	Impact Channels	Impact entry module
FRoL	Failure Rate of Loans	Economy
LaPr	Labour Productivity	
GovSp	Government Spending	
En	Energy Demand (change in cooling and heating demands)	Energy
	Power plant efficiency	
	Energy Infrastructure	
ClimExHB	Climate Extreme risk perception on Human Behaviour	Food Demand
	Sea Level Rise effects on climate extreme risk perception	
Mortality	Mortality	Demography
	Sea Level Rise effects on fatalities	
DuCn	Durability of Concrete	Resources
	Sea Level Rise effects on infrastructure	
CrFw	Crop Yield	Land use and Agriculture

https://doi.org/10.5194/egusphere-2026-3072
Preprint. Discussion started: 1 July 2026

	Freshwater	
SLR	Sea Level Rise effects on failure rate of loans	Economy
	Sea Level Rise effects on productivity	
	Sea Level Rise effects on relocation costs	
	Sea Level Rise effects on protection costs	
AllImpacts	EMB (with all climate impacts)	
NoImpacts	Counterfactual (without any climate impacts)	

2.5 Uncertainty estimates

To quantify the uncertainties in the projections of the single-channel experiments, we use the same sampling approach as done for the EMB projection, reported in Schoenberg et al. (2025a) and Wells et al. (2026). An ensemble of 100,000 realisations was generated, each representing a unique set of model parameters and hence a possible version of the system behaviour. The sampling approach compares the model output to observations and assigns likelihoods based on how well the simulations reproduce the past measurements, based on the assumption that the residuals are independently and identically distributed with constant variance. Because the model is nonlinear and does not allow an analytical solution for parameter uncertainty, the best-fit parameter values and associated uncertainty ranges were determined numerically via internal calibration using literature-based ranges when possible or subject matter expert-decided ranges when none other were available. Simulations were assigned likelihoods based on the extent to which they fit the calibration data. The distribution of outputs from the ensemble was used to derive confidence bounds on model projections at each time point, providing a deterministic measure of uncertainty.

3 Results from the impact experiments

The results from the experiments summarised in Table 2 are structured into three subsections. Section 3.1 outlines the differences between the AllImpacts and NoImpacts projection. Section 3.2 focuses on the role of individual climate–to–society impact channels in shaping the transition between the NoImpacts and AllImpacts projections for key variables. Finally, Section 3.3 examines how these impacts feed back into the climate system.

3.1 The counterfactual (NoImpacts) versus the EMB (AllImpacts) run

In this section we compare the EMB ensemble to the counterfactual ensemble without the climate impacts. Figure 4 presents FRIDA's behaviour without exogenous forcing i.e. policy, its EMB set of runs, here termed AllImpacts as it incorporates the

https://doi.org/10.5194/egusphere-2026-3072
Preprint. Discussion started: 1 July 2026

set of impact channels modelled in FRIDA —alongside a counterfactual case without any climate impacts, termed NoImpacts (Table 2), for key indicators representing the model's six modules. The NoImpacts run starts from 1980 and thus deviates from the history (which has experienced a certain level of climate impacts), to which the FRIDA model has been calibrated (Schoenberg et al., 2025a).

The EMB ensemble, due to the climate impacts structured in FRIDA, produces a different outcome than the NoImpacts projection which deactivates this structure. Disabling climate impacts in FRIDA (red curves in Figure 4) yields substantially higher economic output, as reflected in real per capita GDP (2021 USD; Figure 4a). This economic development translates into greater worker productivity (Figure 4b) and increased public expenditure (Figure 4c).

Demographically, the NoImpacts projection projects a faster growing population (Figure 4d), driven primarily by a marked decline in mortality (Figure 4e). Changes in birth rates are comparatively small and remain within overlapping uncertainty bounds (Figure 4f).

Stronger economic performance combined with a larger population amplifies overall consumption and demand. This is evident in rising energy use (Figure 4g), food demand (Figure 4h), infrastructure expansion, proxied by annual concrete production in FRIDA (Figure 4i), and higher agricultural output, including crop yields and agricultural water use (Figure 4j–k). These socioeconomic changes substantially increase greenhouse gas (GHG) emissions (Figure 4l), resulting in approximately 1°C additional median warming by 2150 (Figure 4m) under the NoImpacts projection. The associated increase in radiative forcing and surface temperature anomaly drives a median increase of global mean sea-level rise of about 0.25 m by 2150 (Figure 4n).

https://doi.org/10.5194/egusphere-2026-3072
Preprint. Discussion started: 1 July 2026

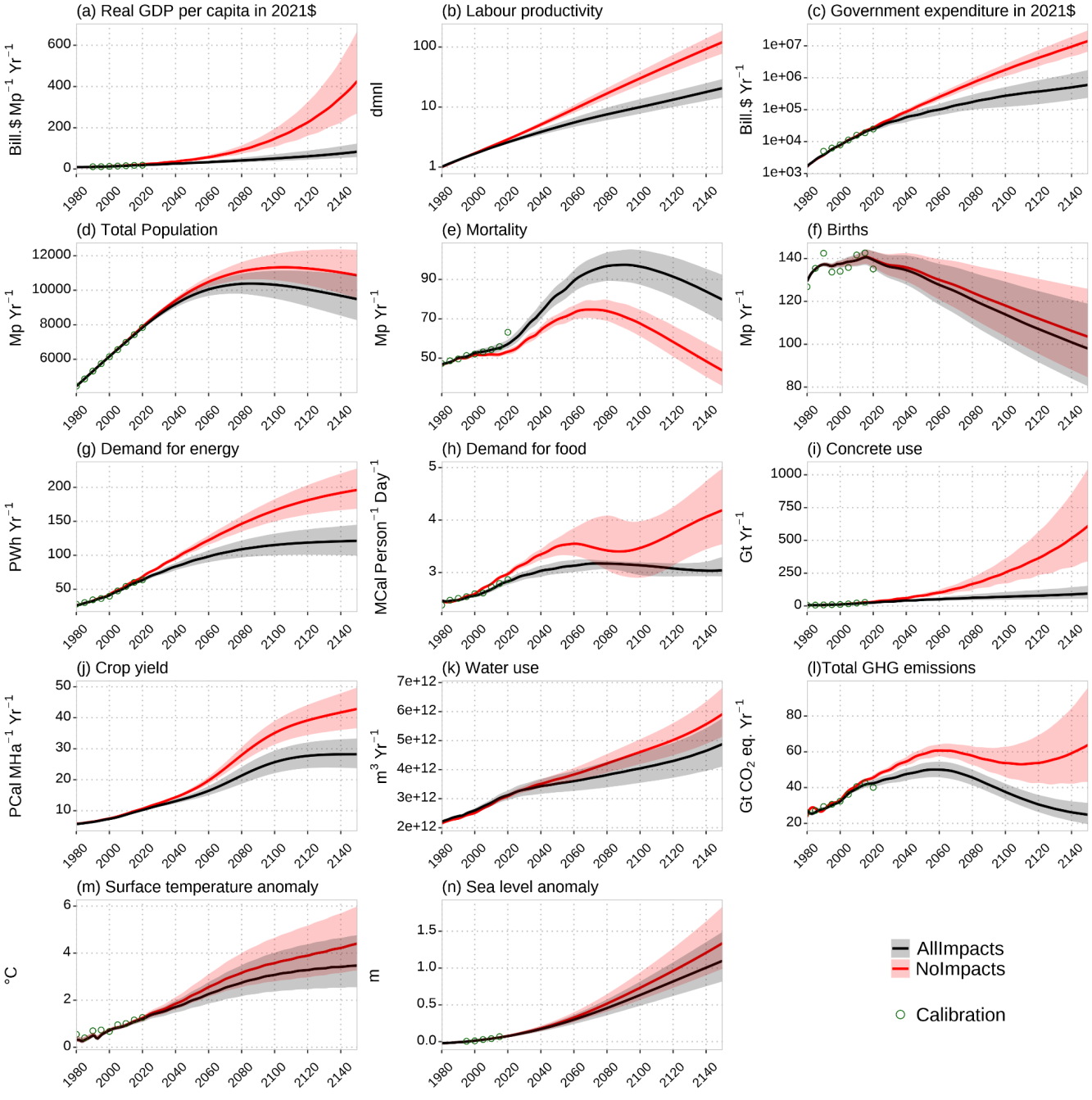

Figure 4: Model behaviour in FRIDAv2.1 with (in black) and without (in red) climate impacts. The solid line indicates the median of a 100,000 member ensemble and the shaded region indicates 67% uncertainty bound. Green circles indicate the data that the model was calibrated to.

https://doi.org/10.5194/egusphere-2026-3072
Preprint. Discussion started: 1 July 2026

3.2 Impacts of the climate feedbacks onto FRIDA's societal modules

This section explores how the individual climate impact categories shape trajectories of key indicators of the six anthropogenic modules in FRIDA, as shown in Figure 4, through the corresponding feedback mechanisms. Impacts are classified as primary, secondary, or marginal, based on the magnitude of their effects.

3.2.1 Economy

The economy module of FRIDA v2.1 (Grimeland et al., 2026) is a Schumpeterian (Schumpeter, 1934), disequilibrium model of endogenous growth that integrates monetary and financial dynamics, innovation-driven productivity, and endogenous business cycles within climate constraints. By replacing aggregate damage functions with disaggregated, empirically grounded mechanisms, it enables explicit analysis of climate-finance interactions, transition risks, and long-run macroeconomic consequences, demonstrating how climate impacts propagate through investment, financial stability, and public budgets (Schoenberg and Callegari, 2025). The climate impacts in FRIDA that directly interface with the economy are: climate-related bankruptcies, labour productivity reductions, government expenditure impacts, and sea level rise–related costs (Ramme et al., 2025; Wells et al., 2026).

In response to increased bankruptcies, banks raise their lending standards, decreasing credit availability, investment and therefore overall economic growth (Dell'Ariccia and Marquez, 2006; Fishman et al., 2024; Lown and Morgan, 2006; Rodano et al., 2018; Schoenberg and Callegari, 2025). The default rate, defined as the share of issued loans that are not repaid (World Bank, 2023), is driven by banks' lending standards, the availability of productive investment opportunities in the economy (proxied by the ratio of investment growth to real GDP growth), and, to a lesser extent, changes in surface temperature anomaly representing climate-related risks such as extreme weather events (Schoenberg and Callegari, 2025).

In normal operations, the banks' responses of raising lending standards to counteract increases in defaults ameliorates the fundamental issue driving defaults, namely the relative lack of good investment opportunities, via the feedback loops generated by *direct* and *indirect lending standards impact* in Figure 2 (B1 and B2). However, raising lending standards does not adequately address the causes of climate change, turning this response into a maladaptation when climate change contributes significantly to defaults (Schoenberg and Callegari, 2025). By raising lending standards in response to climate driven defaults (experiment *FRoL*, Table 2), banks suppress investment, leading to cascading effects, including diminished innovation capacity, a rising debt–to–GDP ratio, which constrains government expenditures, and lower labour productivity. These cascading processes ultimately reduce mitigation efforts creating a reinforcing spiral that diminishes the capacity of the system to adapt to climate change (Schoenberg & Callegari, 2025), expressed by the loop *investments on climate* in Figure 2 (loop R1). Owing to the reinforcing nature of this process, climate–driven increases in loan defaults progressively dominate other impact channels. Figure 5 reflects this behaviour in terms of the widening divergence between trajectories of key economic indicators, spanning real GDP per capita (Figure 5 a, b), worker productivity (Figure 5 c, d), and government expenditure (Figure 5 e, f).

https://doi.org/10.5194/egusphere-2026-3072
Preprint. Discussion started: 1 July 2026

Productivity growth in FRIDAv2.1 arises from two sources of investment: exploratory lending that finances entrepreneurial market entrants and innovation undertaken by incumbent firms (Grimeland et al., 2026). Exploratory lending increases when investment activity outpaces GDP growth, reflecting the expansion of credit toward innovative ventures, while incumbent firms adjust their innovation efforts in response to profitability conditions. These exploratory lending and innovation activities generate potential productivity gains, which materialise as realised labour productivity after a time delay reflecting the period required for innovations to produce observable impacts on economic output. Gains in realised productivity support higher economic output and profitability, which in turn stimulate further investment and innovation. This creates a reinforcing innovation-based growth dynamic, represented by the feedback loop *innovation-driven productivity gain* (loop R2) in Figure 2.

The incorporation of climate impacts on labour productivity (Experiment *LaPr*, Table 2) captures direct productivity damages due to climate change (Dasgupta et al., 2021). As the temperature rises, productivity declines in proportion to workers' exposure to climate. High-exposure labour, such as strenuous outdoor work, is most affected; low-exposure labour, such as shaded but non-climate-controlled tasks, is moderately affected; and no-exposure labour, such as work in climate-controlled offices, is unaffected. To capture this, the model tracks the distribution of labour across three main economic sectors—agriculture, industry, and services—and assigns each sector shares of high, low, and no exposure work. Agricultural labour is the most sensitive to climate impacts, followed by industry, with the service sector being least affected. The overall reduction in labour productivity is derived as a weighted average across sectors (Wells et al., 2026), reflecting their share of the global economy. These effects propagate through the feedback loop *climate-driven productivity loss* (loop B3) as shown in Figure 2 to diminish overall productivity and hence the economic output.

This pathway exerts secondary effects on the economy, as it accounts for roughly 10% of total productivity losses (Figure 5 d) in the median, while most of the remaining productivity losses arise via climate-driven loan defaults transmitted through the GDP per capita described earlier (Experiment *FRoL*, Table 2).

FRIDA captures the societal impacts of sea level rise driven by climate change (Ramme et al., 2025), including coastal flooding, associated mortality, behavioural responses, and infrastructure damages, as well as economic consequences such as relocation and protection costs, productivity losses due to increased coastal exposure, and defaults of otherwise safe loans. The societal consequences of sea level rise are represented through the impact channels *Mortality*, *ClimExHB*, and *DuCn* (Table 2). The *SLR* impact channel primarily captures the financial consequences of sea level rise.

In the absence of sufficient adaptation, sea level rise-induced damages increase the probability of investment failures, reducing productive capital formation. Lower investment leads to declines in output, which in turn reduce wages and bank profits (Grimeland et al., 2026), generating productivity losses (CLD in Figure 2 and Figures 5c–d). This contraction in economic activity diminishes the tax base and government revenues, leading to lower public expenditure to avoid rising debt levels (Figures 5e,f), which further reinforces reductions in output and investment. Overall, the SLR impact channel introduces a dampening mechanism in the economy, offsetting otherwise reinforcing growth dynamics observed in the NoImpacts simulation.

https://doi.org/10.5194/egusphere-2026-3072
Preprint. Discussion started: 1 July 2026

The next-largest contribution to economic damages arises from the climate-induced government spending, which captures increasing maintenance and repair costs, represented as public expenditure in Figure 5e and 5f, stemming from heightened damage to critical infrastructure such as power grids, bridges, and dams (Wells et al., 2026). As temperature-driven public spending increases, the capital available for public investment gradually reduces, leading the government to assume additional debt, which eventually raises the debt-to-GDP ratio and constrains public spending (Grimeland et al., 2026). This interaction is formalized through the balancing feedback loop *debt-driven Govt. spending*, B4, in the CLD (Figure 2). The net effect on economic growth and other model variables depends on the trade-off between GDP gains and inflation associated with higher government spending, and GDP losses resulting from reduced investment due to the government attempting to balance its budget. The modest post-2080 increase in real GDP per capita (Figure 5a) driven by temperature-induced changes in government spending reflects this trade-off.

Inflationary pressures arising from direct climate impacts on energy demand through the channel *En*, driven by imbalances between the growth rates of energy supply and demand result in a persistent but marginal downward trend in the economic indicators shown in Figure 5. In contrast, climate impacts on human behaviour, mortality, and concrete use exert negligible individual effects on these indicators and are therefore omitted from the figures.

https://doi.org/10.5194/egusphere-2026-3072
Preprint. Discussion started: 1 July 2026

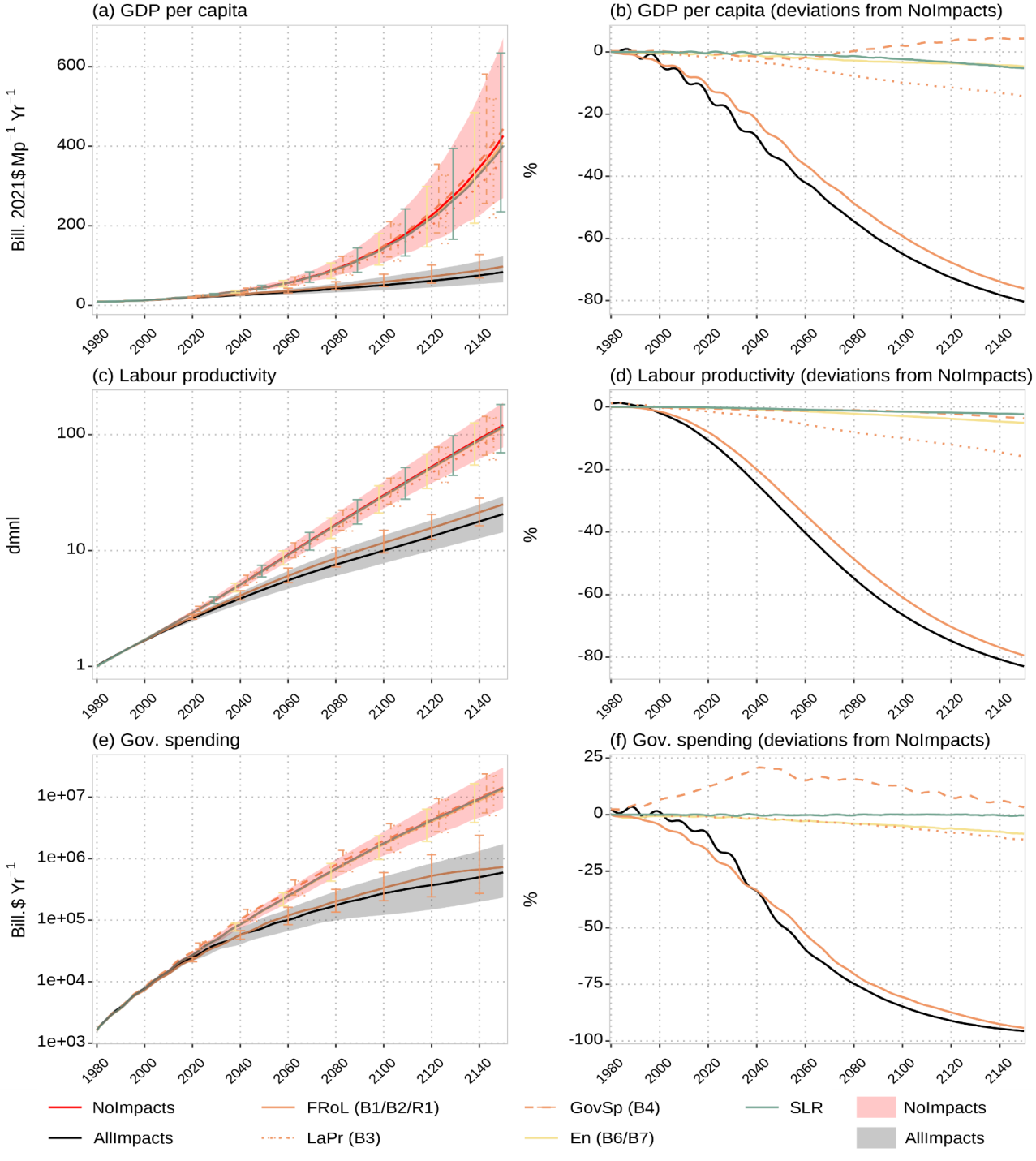

Figure 5: Sensitivity of key economic indicators represented by (a) GDP per capita, (c) labour productivity, and (e) government spending in FRIDAv2.1 in the baseline (AllImpacts) projection with all the climate impacts (solid black lines), the NoImpacts projection (solid red lines) and for individual climate–driven impact channels, represented by

https://doi.org/10.5194/egusphere-2026-3072
Preprint. Discussion started: 1 July 2026

the solid lines with the colour coding from Figure 1. The impacts on the economy are distinguished by solid (*FRoL*), dotted (*LaPr*), and dashed (*GovSp*) lines of the same colour. The shaded area and the error bars in the left panel indicate the 67% uncertainty range represented by a 100,000–member FRIDA simulation. The error bars shown in the left panel (a, c, and e) correspond to different years for the single-channel experiments with a jitter factor of 3 years between the experiments. The right panels (b, d, and f) show the effects of the climate impacts highlighted in the left panels as medians of the corresponding deviations from the counterfactual case in percent (same colour coding as in their absolute behaviour on the left panels). Letters within the parentheses in the legend labels represent feedback loops (shown in Figure 2) through which the corresponding individual impact channels enter the model system.

3.2.2 Demography

In FRIDA, the demography module captures the evolution of age-based population cohorts via births and mortality (Schoenberg et al., 2025a). Births are governed by the female fertility rate, which is endogenously linked to GDP per capita, forming a reinforcing feedback structure (loop R3 in Figure 2). Rising living standards and increased female literacy reduce fertility (Kirk, 1996; Lesthaeghe, 2010; Marquez-Ramos and Mourelle, 2019; Proto and Rustichini, 2013). Lower fertility, in turn, raises real GDP per capita through its effects on employment and the dependency ratio. Mortality is driven by GDP per capita, reflecting the relationship between increased standards of living and mortality (Preston, 1975; Deaton, 2003). The effects of climate change, formed by rising temperature and SLR–related flooding exposure in coastal populations, further modulates the dynamics of these. Rising STA affects mortality by increasing (decreasing) extreme hot-related (cold-related) deaths (Wells et al., 2026), with a skewed distribution towards the old–aged population (Chen et al., 2024). The implementation of this impact channel reflects the dominant influence of rising hot-related mortality, which outweighs the declining cold-related mortality (Cromar et al., 2022).

Figure 6 displays the response of mortality to different climate impact categories. Introducing climate impacts leads to a markedly higher mortality rate in the EMB scenario (red to black line, Figure 6a), mainly driven by economic effects of climate change that propagate through the loan-failure mechanism via feedback loop *investments on climate* (R1, Figure 2). Direct temperature effects on mortality play a secondary role by modifying the balancing loop *mortality impact* (B5, Figure 2). The loops *climate-driven productivity loss* and *debt-driven Gov. spending* exert a comparatively smaller influence on demographic dynamics, relative to the effects transmitted through the temperature-driven and indirect economic mechanisms.

Mortality peaks around 2080 in the AllImpacts projection, with individual climate channels peaking about two decades earlier. This shift emerges from long-term fertility decline—driven by rising literacy and economic growth—reducing population and total mortality. This transition is shaped by the evolving dynamics and interconnections between the balancing and reinforcing loops corresponding to birth and mortality impacts indicated by Figure 2.

https://doi.org/10.5194/egusphere-2026-3072
Preprint. Discussion started: 1 July 2026

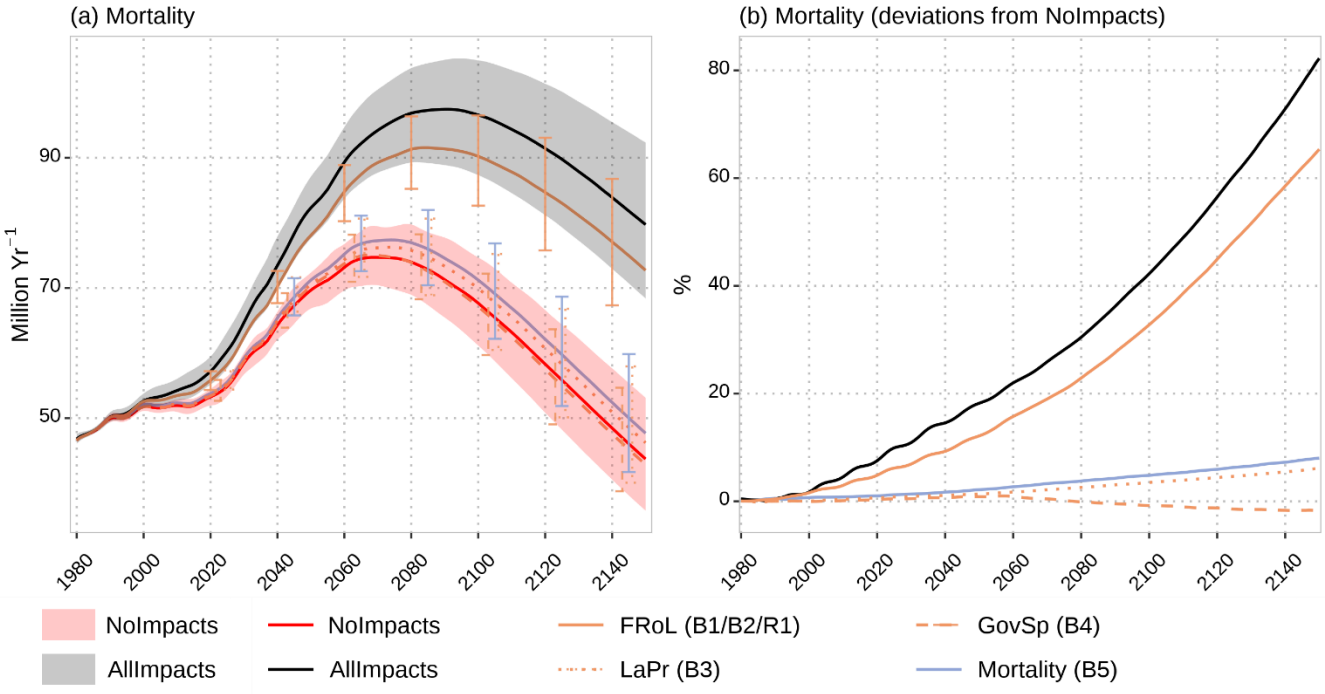

Figure 6: FRIDA's behaviour in terms of mortality in different experiments (Table 2). Characters within the parentheses refer to the specific loops (identified in Figure 2) through which the corresponding impact channels modify mortality. Shaded areas and error bars in (a) represent 67% uncertainty range.

3.2.3 Energy

FRIDA represents multiple global energy sources. Direct climate impacts on the energy sector are temperature–driven and operate directly via three channels:

1. **Shifts in energy demand** from changing heating and cooling needs, captured via heating and cooling degree days, with average global Heating Degree Days (HDDs) declining and Cooling Degree Days (CDDs) increasing with increasing global average temperatures (Auffhammer et al., 2017; Kennard et al., 2022; Deroubaix et al., 2021).
2. **Efficiency losses in thermal and hydropower plants** due to rising water temperatures in power plants and altered streamflows, lowering energy output (Van Vliet et al., 2016).
3. **Infrastructure damage from climate extremes**, which directly reduces energy supply.

These direct mechanisms are captured by the impact channel *En* in the CLD shown in Figure 3 (see also Table 2). Figure 7 illustrates how both direct and indirect climate impacts influence energy pathways in FRIDA.

Overall, the direct climate impacts within the energy module reduce energy demand relative to the NoImpacts projection (red to yellow lines in Figure 7a). This net decline results from two main mechanisms; 1) climate change alters energy needs by

https://doi.org/10.5194/egusphere-2026-3072
Preprint. Discussion started: 1 July 2026

increasing cooling demand while reducing heating demand. The uncertainty range in FRIDA includes both possibilities, though the median projection indicates a slight decrease in total energy demand (Figure 7b); 2) climate–driven damage to energy infrastructure and reduced power-plant efficiency.

Energy investments evolve in response to the mismatch between energy supply and demand, represented by the term *energy deficit* in Figure 3. Climate–driven changes in heating and cooling needs affect this balance. When the increase in cooling demand exceeds the reduction in heating demand, total energy demand rises, creating a supply shortfall. This deficit triggers additional investment in the energy sector across multiple sources—including solar, wind, hydropower, biofuels, nuclear, and fossil fuels—to expand energy capacity. Conversely, when the reduction in heating demand outweighs the increase in cooling demand, overall energy demand declines, reducing the supply–demand mismatch and lowering the need for further investment as existing supply becomes sufficient.

Rapidly expanding energy capacity through higher investments increases the marginal cost of energy production in the short term, which raises energy prices and dampens energy demand. In the longer term technological improvements through learning–by–doing decrease marginal energy costs, with the associated possibility of rebound effects increasing energy demand. These dynamics operate through balancing feedbacks driven by *supply–* and *demand–driven* constraints (loops B6 and B7 in Figure 3). The evolving mismatch between supply and demand influences inflation. Subsequent changes in real GDP per capita feed back into the system adjusting energy demand, forming a closed feedback structure.

The direct climate-driven drop in energy demand only accounts for a median change of ~2–3% in 2100 (Figure 7b). Given that energy demand in FRIDA is driven by real GDP per capita (Schoenberg et al., 2025a), much of the decrease in energy demand from climate change comes about indirectly because of the reduction in economic output. As described in section 3.2.1, the primary cause of loss of GDP is the climate-induced loan defaults and investment failures (via the reinforcing loop *investments to climate*; Figure 2) followed by the loss of productivity due to labour exposure to increasing temperatures (via balancing loop *climate-driven productivity loss*).

Apart from these climate impacts, energy demand is also marginally impacted by climate impacts on crops and freshwater due to the limited role that biofuels play in supplying global energy demand (see Section 3.2.6). These marginal effects slightly increase energy supply and reduce production costs, thereby modestly raising energy demand, as illustrated by Figure 7b.

https://doi.org/10.5194/egusphere-2026-3072
Preprint. Discussion started: 1 July 2026

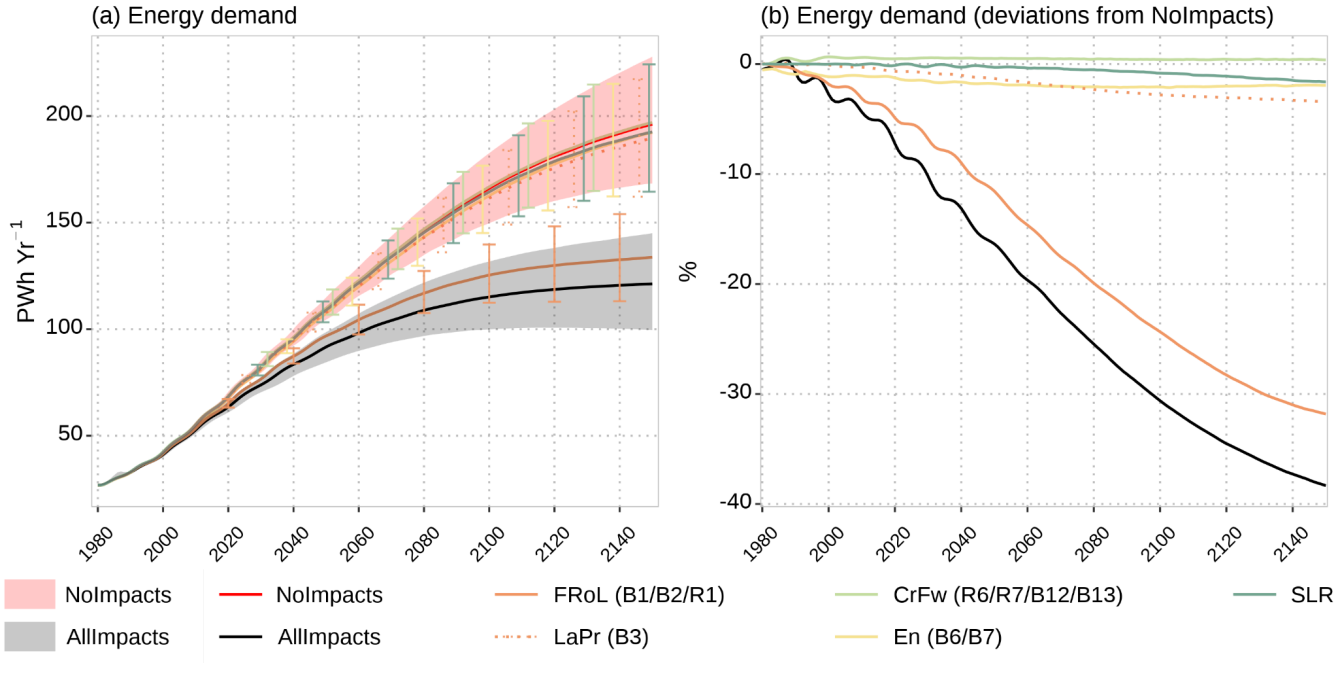

Figure 7: FRIDA's behaviour in terms of energy demand in different experiments (Table 2). Characters within the parentheses refer to the specific loops (identified in Figure 2 and 3) through which the corresponding impact channels modify energy demand. Shaded areas and error bars in (a) represent 67% uncertainty range.

3.2.4 Behavioural change

The behavioural change module in FRIDA (Rajah et al., 2025) represents the complex feedback processes within the human–climate system that determine shifts in dietary preferences. These shifts, disaggregated into animal– and plant–based products, are modelled in Rajah et al., (2025) as a function of distinct behavioural motivations—personal norms, descriptive social norm, and accessibility—constrained by past behaviour and affordability.

Climate impacts modify the demand–side human behavioural responses through the loops *health value-driven personal norm*, *social value-driven personal norm*, *social value-driven descriptive norm*, and *constraint from scarcity* shown in the CLD in Figure 3. These feedback loops are associated with the three normative concepts, modulated by the climate impacts, primarily through real GDP per capita and secondarily through changes in demand through shifts in personal norms.

Personal norms are standards that people hold and expect of themselves, shaped by perceptions of the socio–ecological ways of acting (Bamberg and Möser, 2007). The perceived social value is determined partly by a long–term consumption trend, which exerts a reinforcing effect on consumption and demand, as reflected by feedback loop *social value–driven personal norm* in Figure 3. Subsequent overconsumption poses increased concerns over its adverse effect on health and forces people to consume less, causing a balancing effect on demand reflected by the loop *health value–driven personal norm* in Figure 3.

https://doi.org/10.5194/egusphere-2026-3072
Preprint. Discussion started: 1 July 2026

Descriptive norms are guided by the dynamic shifts in the social environment that provide motivation for people to conform (Cialdini, 2007; Cialdini et al., 1991; van Valkengoed et al., 2025). These shifts are largely near–term, as people do not have perfect information on the long-term trend within a social environment (Rajah et al., 2025). This process produces a reinforcing mechanism on consumption, and hence demand, due to the "preconformity" to social behaviours (Sparkman and Walton, 2017), indicated by the loop *social value-driven descriptive norm* in Figure 3.

The third behavioural motivation, accessibility, is guided by a perception of socio–economic factors, encompassing income, price of the food products and economic development (Godfray et al., 2018; Milford et al., 2019). Food prices are parameterised by a factor reflecting scarcity in food products, fluctuated by relative supply–demand balance between animal and crop products (Rajah et al., 2025). When the production of animal products is higher relative to that of crop products, its availability increases, thus decreasing the food scarcity. As a result, the demand from accessibility rises leading to a change in the total food demand in the same direction. As demand rises, the availability (scarcity) goes down (up), producing a balancing loop, *constraint from scarcity* (Figure 3), on the total food demand.

The effects of these loop modulations from climate impacts can be seen in the behavioural plots in Figure 8. The introduction of climate impacts brings the food demand substantially down from the NoImpacts case (red to black curve, Figure 8a). Climate impacts enter the behavioural module from 3 directions–through the accessibility parameter shaped by real GDP per capita, the direct impact on personal norms through the perceived climate change risk, and the changes in crop yield caused by the impact channels on energy (through changes in biofuel production) and land use (see section 3.2.6). The former two channels produce the primary and secondary impacts respectively, with the effect of changing crop yield on food demand being a relatively lower–order impact.

Climate–induced loan defaults is by far the strongest mechanism driving the food demand, as indicated by Figure 8b, due to its dampening effect on real GDP per capita (see section 3.2.1), reducing the accessibility of food products, which also shapes the personal and descriptive norms of behaviour. In the absence of these indirect economic consequences, the largest effect comes from the direct climate impact channel, which accounts for the influence of climate extremes on human behaviour. As exposure to climate extremes and sea level rise increases, perceived climate risk rises, activating the balancing loop *climate risk–driven personal norms* (loop B9, Figure 3). This shift in norms reduces consumption and leads to a decline in food demand, as reflected in the *ClimExHB* experiment (Figure 8b). However, toward the end of the century, demand begins to rebound, indicating adaptation to a warmer "new climate normal" and a degree of climate desensitization (Alhadeff, 2015). This recovery is further supported by the self-correcting *health value–driven personal norm* (loop B8, Figure 3), as reduced consumption lowers perceived health risks over the long term. Food demand therefore evolves through interacting reinforcing and balancing feedback loops, driven by changes in perceived risk-signals and long-term consumption patterns.

https://doi.org/10.5194/egusphere-2026-3072
Preprint. Discussion started: 1 July 2026

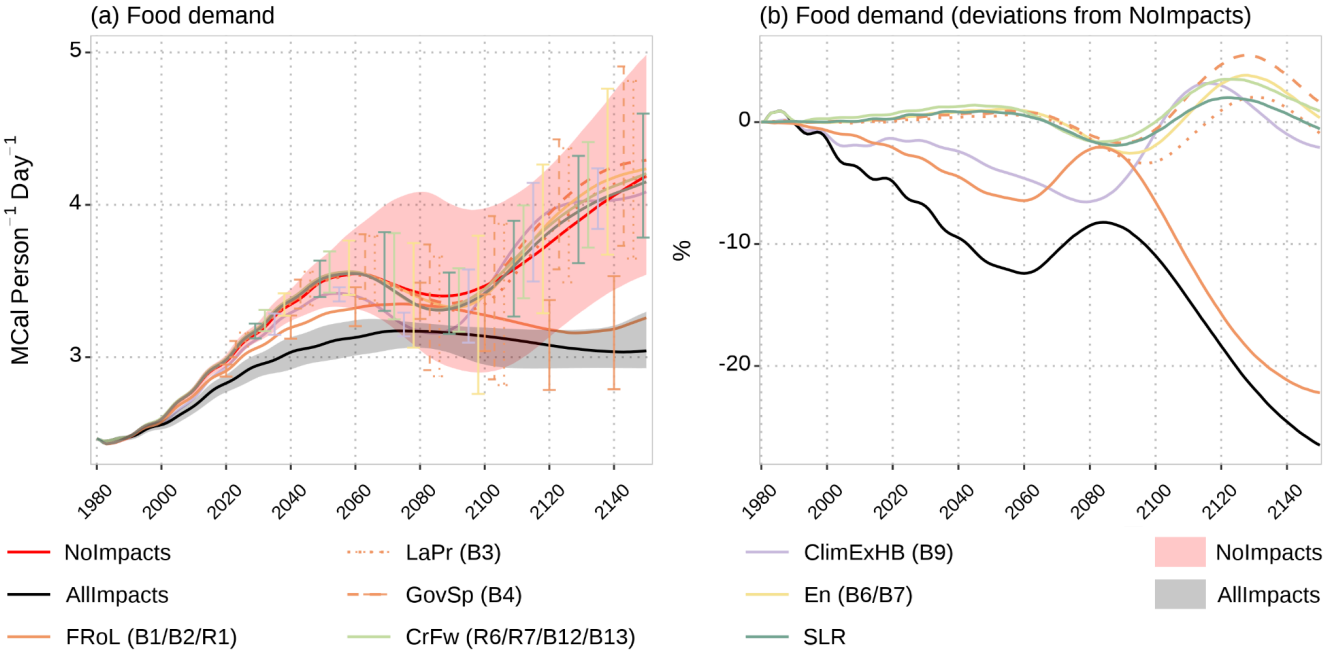

Figure 8: FRIDA's behaviour in terms of total food demand in different experiments (Table 2). Characters within the parentheses refer to the specific loops (identified in Figure 2 and 3) through which the corresponding impact channels modify food demand. Shaded areas and error bars in (a) represent 67% uncertainty range.

3.2.5 Resources

The resources module in FRIDA refers to the construction sector, encompassing residential, commercial, and civil infrastructure, modelled via its annual concrete use metric, given that concrete accounts for a substantial portion of the total material stock utilized for construction activities (Deetman et al., 2020). Global concrete production is driven by population and wealth in the associated sectors in FRIDA to model the demand for housing and infrastructure. Following production, the concrete transitions from new to aging infrastructure stocks and exits the system upon the structure's decommissioning at the end of its operational lifetime. This forms a balancing loop, highlighted by the loop *concrete replacement* in Figure 3 (B11), where aging and new construction counter each other.

Figure 9 illustrates the response of the annual concrete production stock when the climate impacts enter the balancing loop *concrete replacement* directly through the durability metric, and indirectly through real GDP per capita. The direct channel linking the concrete usage to climate change captures the reduction of the operational lifetime of concrete structures due to accelerated corrosion in structures led by increased temperature-driven carbonation and chloride penetration (Bastidas-Arteaga and Stewart, 2014; Stewart et al., 2011) as well as the damages caused by flooding from the increased sea level. These damages necessitate higher maintenance and increased concrete production annually, reflected by the curve corresponding to the impact channel *DuCn* in Figure 9b.

https://doi.org/10.5194/egusphere-2026-3072
Preprint. Discussion started: 1 July 2026

Overall, climate impacts reduce concrete production by 40-50% by 2100 and 80% by 2150 (red to black curve, Figure 9a), predominantly due to the drop in real GDP per capita from economic consequences of climate change (Figure 9b). The primary factor in this mechanism is the climate-induced loan defaults, followed by the drop in labour productivity, financial consequences of sea-level rise, and inflationary pressures produced by the differences between energy demand and supply growth rates (see section 3.2.1).

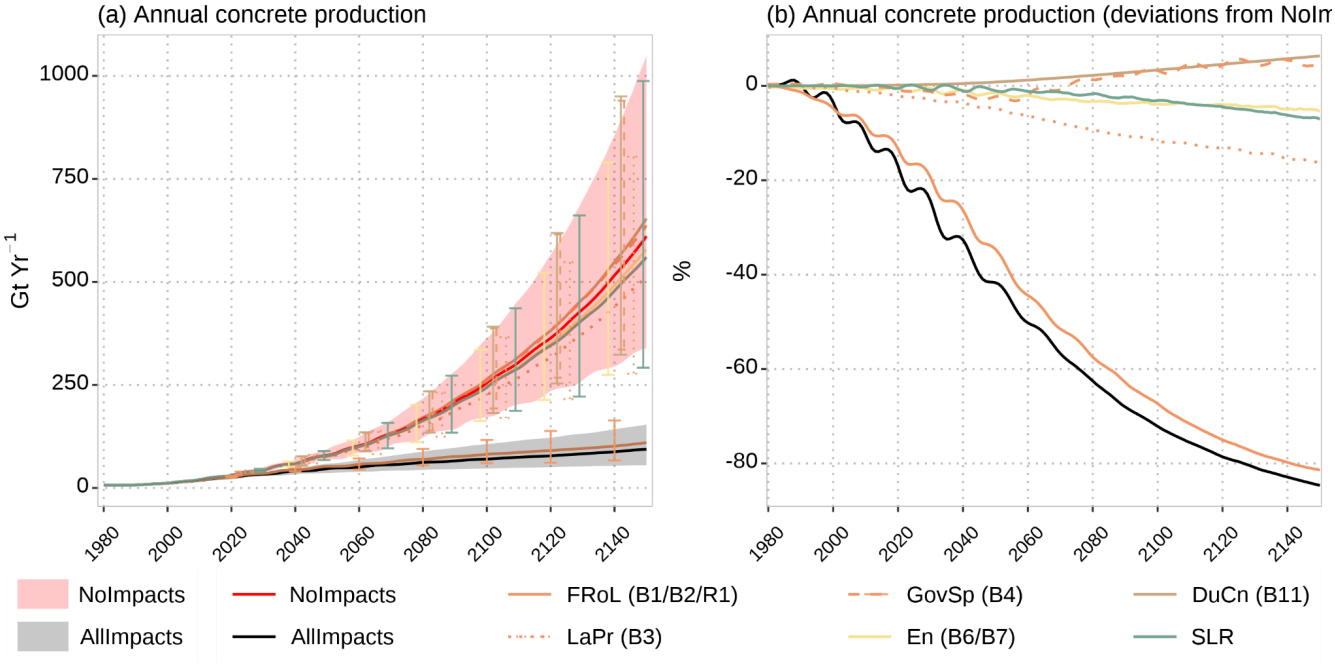

Figure 9: FRIDA's behaviour in terms of annual concrete production in different experiments (Table 2). Characters within the parentheses refer to the specific loops (identified in Figure 2 and 3) through which the corresponding impact channels modify concrete production. Shaded areas and error bars in (a) represent 67% uncertainty range.

3.2.6 Land Use and agriculture

In FRIDA, agricultural productivity is represented by a globally aggregated crop–yield stock (Wells et al., 2026). Climate impacts on crop yield are driven by atmospheric CO_2 concentration and the global mean surface temperature (Figure 1), which propagate through four interacting mechanisms: irrigation responses, temperature effects, CO_2 fertilisation, and fertiliser application (Figure 3).

The direct climate–crop yield pathway operates through irrigation dynamics, temperature effects, and CO_2 fertilisation. Rising temperatures increase evapotranspiration, inducing water stress that reduces irrigation efficiency, as larger water volumes are required to irrigate the same cropland area. This process generates a balancing feedback on crop yield (*irrigation effect,* loop B12, in Figure 3). The strength of this mechanism also depends on real GDP per capita, which reflects technological improvements in irrigation efficiency.

https://doi.org/10.5194/egusphere-2026-3072
Preprint. Discussion started: 1 July 2026

Temperature effects on crop yield follow a quadratic relationship between absolute global mean surface temperature and yield (Franke et al., 2020), resulting in yield gains at lower temperatures and losses at higher temperatures. In contrast, the linear *CO_2 fertilization* mechanism (Franke et al., 2020) creates a reinforcing feedback (loop R6, Figure 3): higher crop yields accelerate cropland degradation, increasing atmospheric CO_2 concentrations and thereby amplifying the fertilization effect. The CO_2 fertilization effect is a key source of uncertainty in the crop yield (Gernaat et al., 2021; Müller et al., 2024) as it depends strongly on crop type and water stress (Ostberg et al., 2018).

The indirect climate effects on crop yield operate through two main pathways. First, an economic pathway links GDP to crop yield via its influence on food demand, which propagates to crop demand, alters the crop balance, and drives cropland expansion. Second, crop yield responds through the fertilizer application mechanism, which adjusts endogenously to imbalances between crop demand and supply via the interacting feedback loops of production-driven and demand-driven fertilizer response. Both pathways are represented in the CLD in Figure 3. Climate impacts enter this structure not directly through the land use and agriculture channel but indirectly cascade through the economic and behavioural pathways that regulate the real GDP per capita and food demand respectively.

Figure 10 displays the effects of the above loops on the evolution of crop yield and agricultural water use. The combined effect of all climate impact channels results in a nearly 30% reduction in crop yields by 2100 relative to the *NoImpacts* projection, as indicated by the solid black line in Figure 9b. The indirect economic impacts, which drive down real GDP per capita via investment failures (see section 3.2.1), exert the strongest balancing influence on the crop yield via the loops *irrigation effect* and *production-driven fertilizer response* (B12 and B13, Figure 3), followed by the climate impacts on labour productivity. The direct climate impact independently produces a marginal impact, generating higher crop yields relative to the *NoImpacts* projection, indicated by the curve corresponding to the channel *CrFw* in Figure 10b.

Secondary impacts on crop yield are produced by the climate–driven changes in energy demand and behavioural norms, through mechanisms distinct from those operating via real GDP per capita. Climate–induced shifts in energy demand and supply (section 3.2.3) increase reliance on biofuel production thereby raising the share of crops allocated to bioenergy and expanding overall crop demand. This perturbation in the crop balance induces higher crop yields via loops *supply–and demand–driven constraint* (B6 and B7, Figure 3), driven primarily by increased fertilizer use. Changes in behavioural norms operate through pathways analogous to those in the energy sector. Shifts in food demand driven by personal norms modify feedback loops in the food demand sector (see section 3.2.4), thereby altering crop demand and, consequently, the crop balance, and hence the fertilizer application.

https://doi.org/10.5194/egusphere-2026-3072
Preprint. Discussion started: 1 July 2026

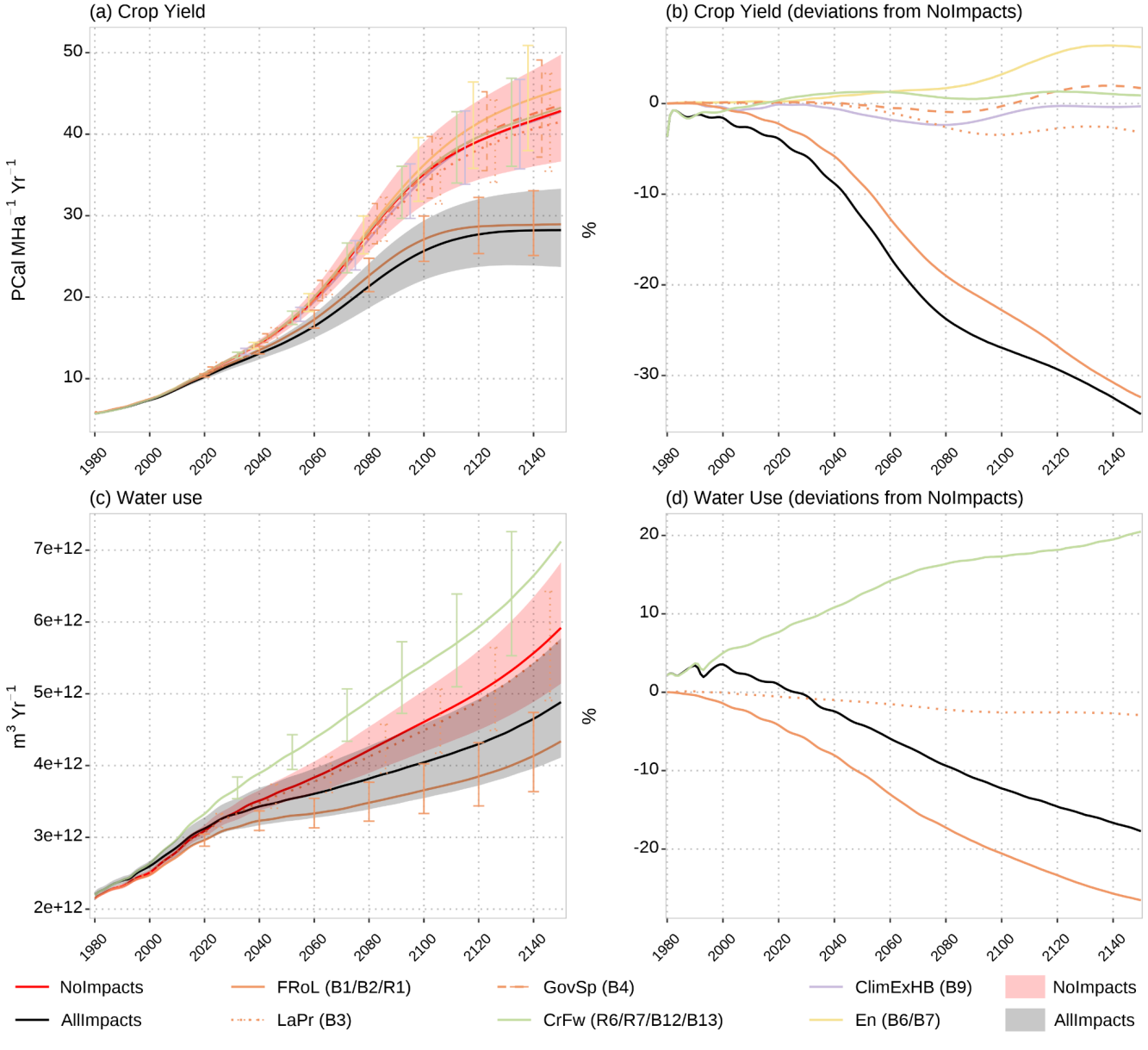

508

https://doi.org/10.5194/egusphere-2026-3072
Preprint. Discussion started: 1 July 2026

Figure 10: FRIDA's behaviour in terms of crop productivity and agricultural water withdrawal in different experiments (Table 2). Characters within the parentheses refer to the specific loops (identified in Figure 2 and 3) through which the corresponding impact channels modify the landuse sector. Shaded areas and error bars in (a) represent 67% uncertainty range.

3.3 Socioeconomic feedbacks on climate

Climate impacts on the socioeconomic system feed back to the climate mainly through adjustments in the emissions, including GHG and non–GHG sources, as depicted by the balancing loop *feedbacks to climate* (B14) in Figure 3. Figure 11 illustrates the total GHG and temperature responses to these socioeconomic feedbacks, indicating the largely balancing effects of the socioeconomic feedbacks on the emissions, producing a median cooling by the individual impact channels.

The overall impact of including climate feedbacks has a strong impact on climate itself, with a median reduction in the warming of about 20% by 2150 (Figure 11b). The pathways through which these feedbacks influence the climate system are diverse. As in other sectors, climate–induced loan defaults and, to a lesser extent, productivity losses account for a large share of the climate response (Figure 11b), primarily through their persistent influence on economic activity, which in turn affects total GHG emissions (Figure 11d) as well as non-GHG emissions emanating from landuse changes and aerosol emissions. Secondary effects arise from direct climate impacts on human behaviour (curve corresponding to the impact channel *ClimExHB*, Figure 11b), which influence CH_4, N_2O, VOC and CO forcings (see Figure 13). Other impact channels exert negligible influence on the climate.

https://doi.org/10.5194/egusphere-2026-3072
Preprint. Discussion started: 1 July 2026

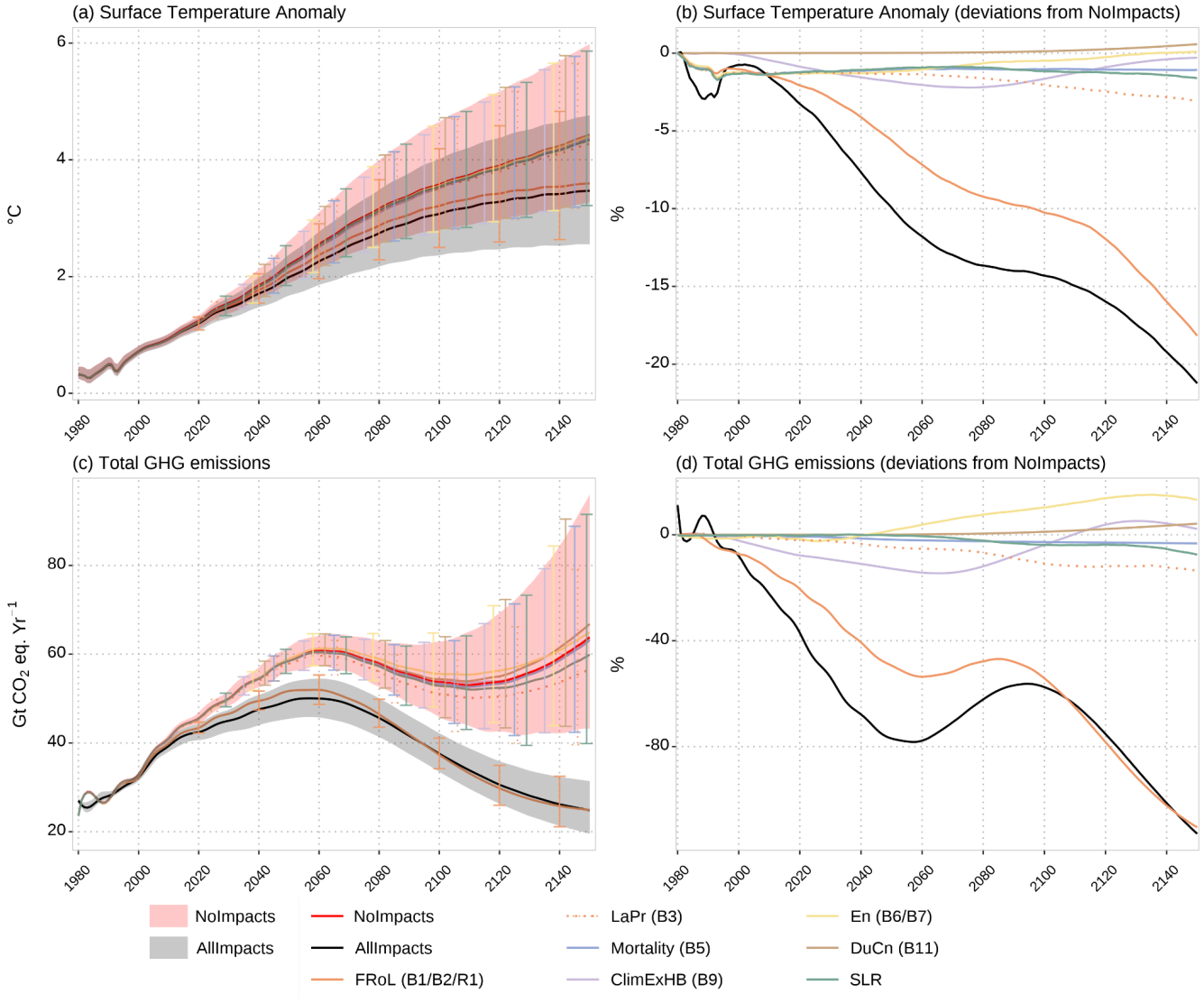

Figure 11: Response of climate, in terms of surface temperature anomaly and total GHG emissions, to individual and fully coupled climate impact channels. Characters within the parentheses refer to the specific loops (identified in Figure 2 and 3) through which the corresponding impact channels modify climate. Shaded areas and error bars in (a) represent 67% uncertainty range.

4 Dominance of climate impacts on the economy, a comparison with DICE

The analysis of the contribution of individual climate impact channels to the endogenous model behaviour of FRIDA v2.1 in Section 3 has shown that a single climate impact channel, climate-induced loan defaults (*FRoL*), dominates the others. Economic impacts emerge as a major pathway through which climate change propagates across sectors, influencing energy demand & supply, human behaviour & food demand, agricultural productivity, concrete production, and so forth. To

https://doi.org/10.5194/egusphere-2026-3072
Preprint. Discussion started: 1 July 2026

contextualize the overwhelming dominance of economic impacts on the system, this section sets up a direct comparison between FRIDA's financial-impact mechanisms and the traditional damage functions used in William Nordhaus's canonical DICE model.

In cost-benefit models like DICE, climate-induced economic impacts are represented using aggregated damage functions that compute losses in production due to the climate change using global mean surface temperature as an input (Nordhaus, 2018; Hope et al., 2013; for a general overview of these approaches, see Bonen et al., 2014 and Diaz and Moore, 2017). In the DICE model, climate damages are incorporated through a damage factor, Ω, that represents a fraction of output remaining after accounting for climate-induced economic losses, expressed by

$$\Omega(t) = \frac{1}{1 + \pi_1 T(t) + \pi_2 T(t)^2} \quad (1)$$

Where T(t) denotes the global mean surface temperature anomaly relative to pre-industrial level, π_1 and π_2 are coefficients calibrated from empirical studies of macroeconomic damages. The inverse form ensures that Ω(t) remains in the range 1 to 0, with the net output decreasing multiplicatively. In practice, the linear coefficient π_1 is set to 0, while the quadratic term π_2 captures the nonlinear growth of damages at higher temperature. In the standard DICE-2016R parameterization (Nordhaus, 2017, 2018), this quadratic coefficient is calibrated to 0.00236, resulting in the operational form,

$$\Omega(t) = \frac{1}{1 + 0.00236 T(t)^2} \quad (2)$$

To compare the economic damages between FRIDA and DICE, the above damage factor is evaluated along the temperature trajectory produced by FRIDA's *AllImpacts* simulation and plotted as the Nordhaus DICE-2016R blue curve in Figure 11. This isolates differences in the representation of damages, as the Nordhaus specification depends only on instantaneous temperature and does not include endogenous growth and financial feedback mechanisms. The median output ratios estimated for FRIDA's *AllImpacts* and *FRoL* experiment ensembles are shown in black and orange, respectively. Notice first that the black and orange lines practically overlap, which is as expected since the *FRoL* climate impact overwhelmingly dominates other climate impact channels. But more importantly, the difference between the blue line and the black/orange lines is both qualitative and quantitative.

https://doi.org/10.5194/egusphere-2026-3072
Preprint. Discussion started: 1 July 2026

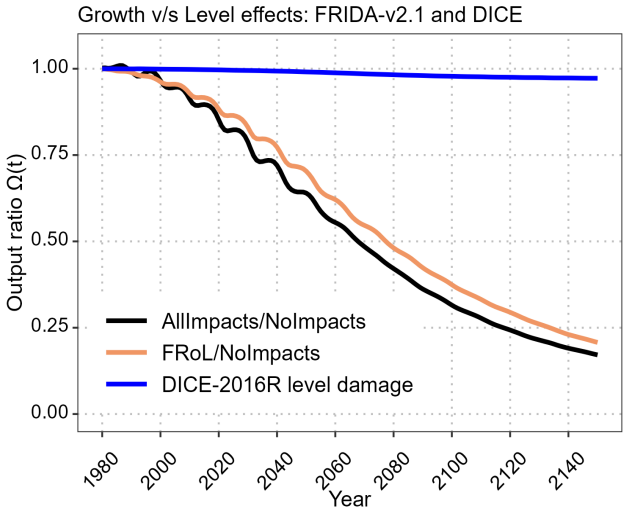

Figure 12: Output ratios (Ω) relative to the FRIDA's NoImpacts projection: full climate impacts (AllImpacts) in black, loan-failure-only impacts (FRoL) in orange. Also shown is the Nordhaus DICE-2016R level-damage specification in blue. All series are computed directly from simulated real GDP trajectories; no additional filtering or detrending is applied. The FRIDA lines are median representatives of the corresponding ensemble.

The qualitative difference between the models relate to the shape of the curves. The DICE output ratio (blue line) declines only modestly and appears to stabilize over time, showing that DICE is a level-damage model. In contrast, FRIDA exhibits a pronounced and persistent decline in the output ratio Ω (black and orange). Because the ratio continues to fall rather than converging toward a constant value, the divergence reflects a sustained reduction in growth rates rather than a one-time proportional reduction in output, implying that FRIDA is a growth-damage model. The quantitative difference between the models relates to the amount of damage: FRIDA exhibits substantially larger levels of damage per degree of warming than DICE (not shown).

5 The importance of nonlinear feedbacks

In the preceding sections, various climate impact channels were examined independently to isolate their specific effects on the system. Here we address the reality that these mechanisms do not operate in a vacuum. Even though economic impacts play a dominant role in determining the outcomes of different model components, the system response cannot be understood by considering individual impacts in isolation. Instead, the impact channels interact through shared state variables and time-delayed mechanisms, generating nonlinear interactions.

To identify such nonlinear interactions, we reproduce figures 5b, 5d, 5f, 6b, 7b, 8b, 9b, 10b, 10d and 11b in Figure 13 with an additional curve representing the sum of all the impact channels (grey lines). Deviations between the grey and black lines indicate that the effects of individual climate impacts do not combine linearly to reproduce the full–impact experiment, implying the presence of non–additive interactions among climate impact channels within the coupled system. A comparison

https://doi.org/10.5194/egusphere-2026-3072
Preprint. Discussion started: 1 July 2026

between the coupled model response (*AllImpacts*) and the additive combination (*sum of individual impacts*) provides a structured way to identify how nonlinearities emerge from the interaction of multiple pathways operating through shared constraints and dynamic feedbacks.

The grey and black lines do not fully overlay each other in any of the model output variables shown in Figure 12. But the non–additive effects vary substantially in strength across variables and over time. The largest deviations between the grey and black lines are observed for food demand (13g), crop yield (13i), agricultural water use (13j), and surface temperature anomaly (13l). In what follows, we show how nonlinearities emerge in these four variables from three ingredients: (i) shared state variables that couple multiple impact channels, (ii) structural constraints such as minimum operators and resource limits, and (iii) dynamic feedback processes and time delays that cause these shared states and constraints to evolve endogenously.

https://doi.org/10.5194/egusphere-2026-3072
Preprint. Discussion started: 1 July 2026

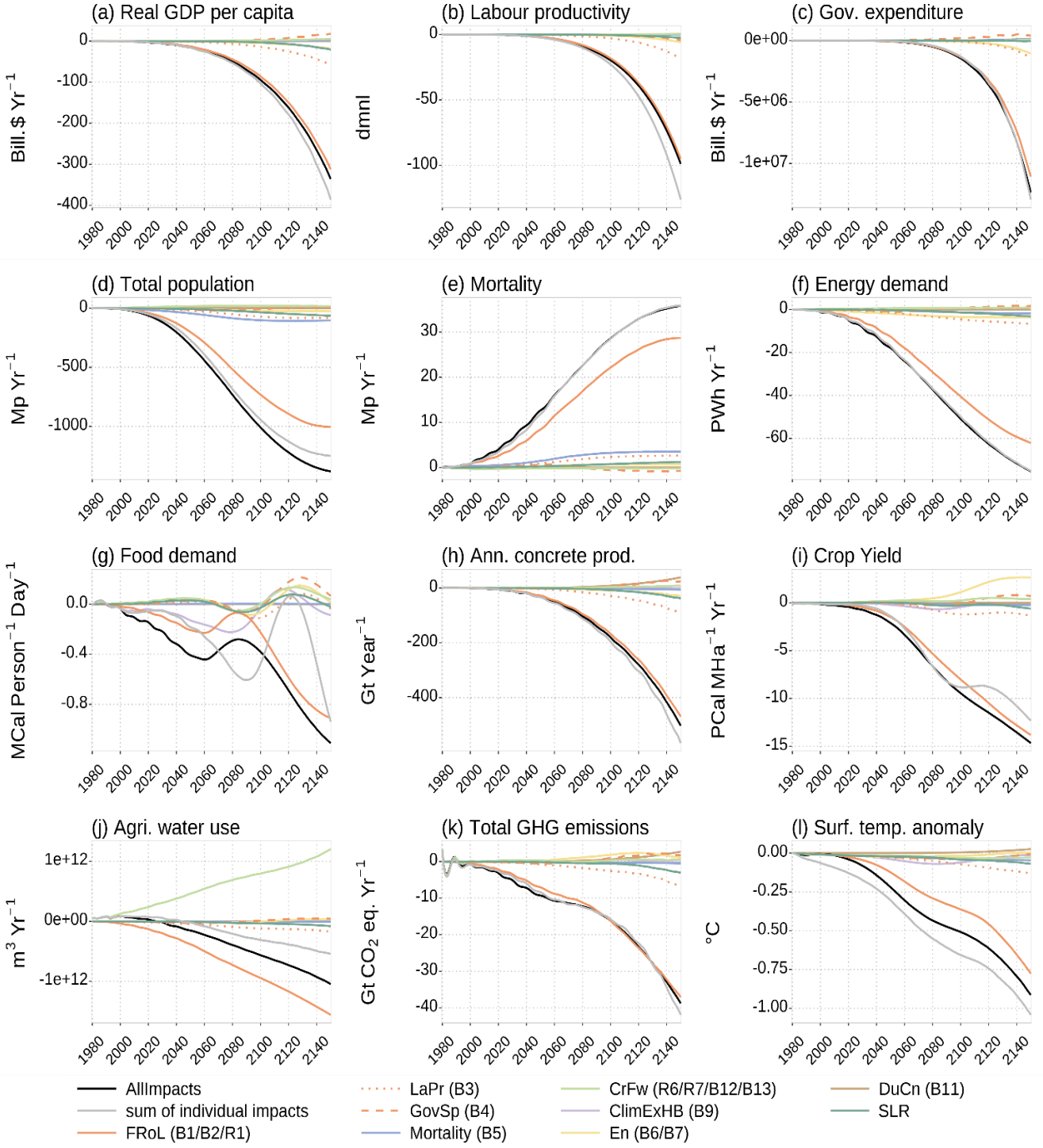

592

https://doi.org/10.5194/egusphere-2026-3072
Preprint. Discussion started: 1 July 2026

Figure 13: Effects of the climate impacts shown as deviations from the *NoImpacts* in absolute values, for (a) Real GDP per capita, (b) Labour productivity, (c) Government expenditure, (d) Total Population, (e) Mortality, (f) Energy demand, (g) Food demand, (h) Annual concrete production, (i) Crop yield, (j) Agricultural Water Use, (k) Total GHG emissions (estimated in CO2 eq. using the Global Warming Potential GWP100 metric), and (l) Global mean surface temperature anomaly. The *AllImpacts* projection is shown as the solid black line, while individual climate impact channels are shown as coloured lines. Impact channels on labour productivity (LaPr) and Government expenditure (GovSp) are indicated by the same colour as that of FRoL, but in dotted and dashed lines respectively, to imply that these are part of the economic module. The solid grey lines represent the sum of the individual impacts. All the lines are median representatives of the 100,000-large ensemble.

5.1 Food demand

Food demand exhibits the strongest nonlinear response in the model because it is governed by two competing mechanisms that can alternate as the binding constraint. Food demand is defined in FRIDA at each timestep as the minimum of two components (using a regime-shifting minimum operator): norm–driven demand (personal and descriptive norms) and accessibility–constrained demand (Rajah et al., 2026). While individual climate impact channels may exhibit approximately linear effects on food demand under isolated perturbations, they do not operate independently in the full coupled system. Rather, they jointly affect a set of shared state variables that determine both components of food demand. These shared variables are GDP, scarcity conditions, perceived social value, and perceived consumption trends. As a result, even when each channel enters these state variables in an approximately additive or locally linear way when considered in isolation, their combined effect becomes non–separable once coupled through the shared system.

Climate impacts on the economy (through investment losses, labour productivity reductions, and fiscal constraints), land use (crop yield and freshwater stress), sea level rise (financial and asset losses), energy systems (infrastructure disruption and demand shifts), mortality (population), climate extreme risk perception (behavioural responses), and infrastructure degradation (concrete durability) all propagate into either or both of the two demand components. The accessibility–driven component responds primarily through GDP, food scarcity, and production constraints, while the norm–driven component responds more slowly through changes in perceived social value, risk perception, and consumption trends shaped by observed conditions and long-term climate and health awareness. These two components therefore evolve under different but interconnected channels of influence.

The resulting interaction structure is further amplified by the five dynamic feedback loops highlighted in Figure 3, *health–value driven personal norm (B8)*, *climate risk–driven personal norm (B9)*, *constraint from scarcity (B10)*, *social–value driven personal norm (R4)*, and *social–value driven descriptive norm (R5)*, two reinforcing and three balancing, that operate through the common state variables perceived social value, demand from accessibility, and perceived consumption trends. Because both demand components are continuously reshaped by these feedback processes, the relative dominance of the norm–driven versus accessibility–driven constraint changes endogenously over time. This creates regime shifts in the structural minimum operator, so that food demand alternates between being norm–limited and accessibility–limited depending on the evolving joint state of the system.

https://doi.org/10.5194/egusphere-2026-3072
Preprint. Discussion started: 1 July 2026

Taken together, (i) multiple climate channels feeding into shared state variables, (ii) feedback–driven co–evolution of those variables over time, and (iii) the regime–shifting minimum operator as a structural constraint imply that food demand is not an additive function of climate impacts. Instead, nonlinearities arise endogenously from the interaction of channels through shared states and from shifts in the binding constraint. Consequently, food demand exhibits stronger nonlinear and cross–channel interaction effects than other model outputs.

5.2 Crop yield and agricultural water withdrawal

Agricultural water withdrawal exhibits the second strongest nonlinearity in the model due to its multiplicative structure and dependence on shared land–water–economic constraints. It is defined in FRIDA as the product of water withdrawal per unit of irrigated cropland and irrigated area. While individual climate impacts may appear approximately linear under isolated perturbations, they jointly affect crop yield and agricultural water use through shared state variables, most importantly cropland availability and water supply. The multiplicative structure implies that simultaneous changes in per-hectare water demand, fraction of irrigated cropland, and cropland stock interact non–additively, such that their combined effect can reinforce or offset total withdrawal depending on how they co-evolve over time. This interaction is further strengthened by temperature-driven increases in evapotranspiration, which raise water demand per hectare and trigger a balancing response through constraints on available water and limits to irrigated area. As a result, agricultural water withdrawal exhibits strong and persistent nonlinearities arising from coupled biophysical processes and land resource constraints, in contrast to the regime–shifting nonlinearity observed in food demand.

Crop yield exhibits a lower but still pronounced nonlinearity, as it depends in part on the fraction of irrigated cropland, which is itself determined by the same shared state variables that govern agricultural water withdrawal, namely cropland stocks and water availability. In addition, yield is directly influenced by climate conditions through nonlinear temperature responses and CO_2 fertilization effects, as well as by fertilizer application. Cropland dynamics further shape yield by determining both total production capacity and the allocation of land between irrigated and rainfed systems. While individual climate impacts on yield may produce approximately linear effects under isolated perturbations, yield becomes nonlinear in the full system because it co–evolves with irrigation decisions, land-use allocation, and fertilizer applications.

These interactions associated with crop yield and agricultural water withdrawal are further strengthened by the propagation of economic impacts of climate change. Investment damages and capital losses reduce productive capacity, while declines in labour productivity and fiscal constraints limit agricultural inputs, particularly fertilizer use and irrigation efficiency. Together, these channels couple economic and biophysical constraints within the same system, amplifying nonlinear responses in crop yield through shared state dependencies and feedback-driven adjustment.

https://doi.org/10.5194/egusphere-2026-3072
Preprint. Discussion started: 1 July 2026

5.3 Surface Temperature Anomaly

The case of surface temperature is particularly interesting because, in the absence of interaction effects across impact channels, the temperature difference between the two experiments (*AllImpacts* and *sum of individual impacts*) would be substantially larger. The nonlinear temperature response arises from heterogeneous responses of greenhouse gas emissions across climate impact channels, which differ in timing, magnitude, and sectoral origin. Although total greenhouse gas emissions appear approximately additive across impact channels (Figure 13k), this aggregation masks important differences in the composition and temporal evolution of individual emission sources (Figure 14). In particular, N_2O and CH_4 emissions, which are strongly linked to the food and land–use sectors, identified as the most nonlinear components of the system (sections 5.1 and 5.2), exhibit distinct responses to climate impacts, contributing to nonlinearities that are not visible in the aggregated emissions signal. These heterogeneous emission pathways generate nonlinear changes in atmospheric concentrations and radiative forcing, which propagate through the carbon cycle and ocean–atmosphere heat exchange system to produce nonlinear temperature trajectories. This is further reflected in the air–sea CO_2 flux, which exhibits a similar nonlinear pattern (Fig. A1), indicating that the carbon cycle itself responds nonlinearly to differences in emissions composition and timing. In addition, inertia associated with ocean heat uptake causes these differences to accumulate over time, further amplifying deviations in surface temperature.

https://doi.org/10.5194/egusphere-2026-3072
Preprint. Discussion started: 1 July 2026

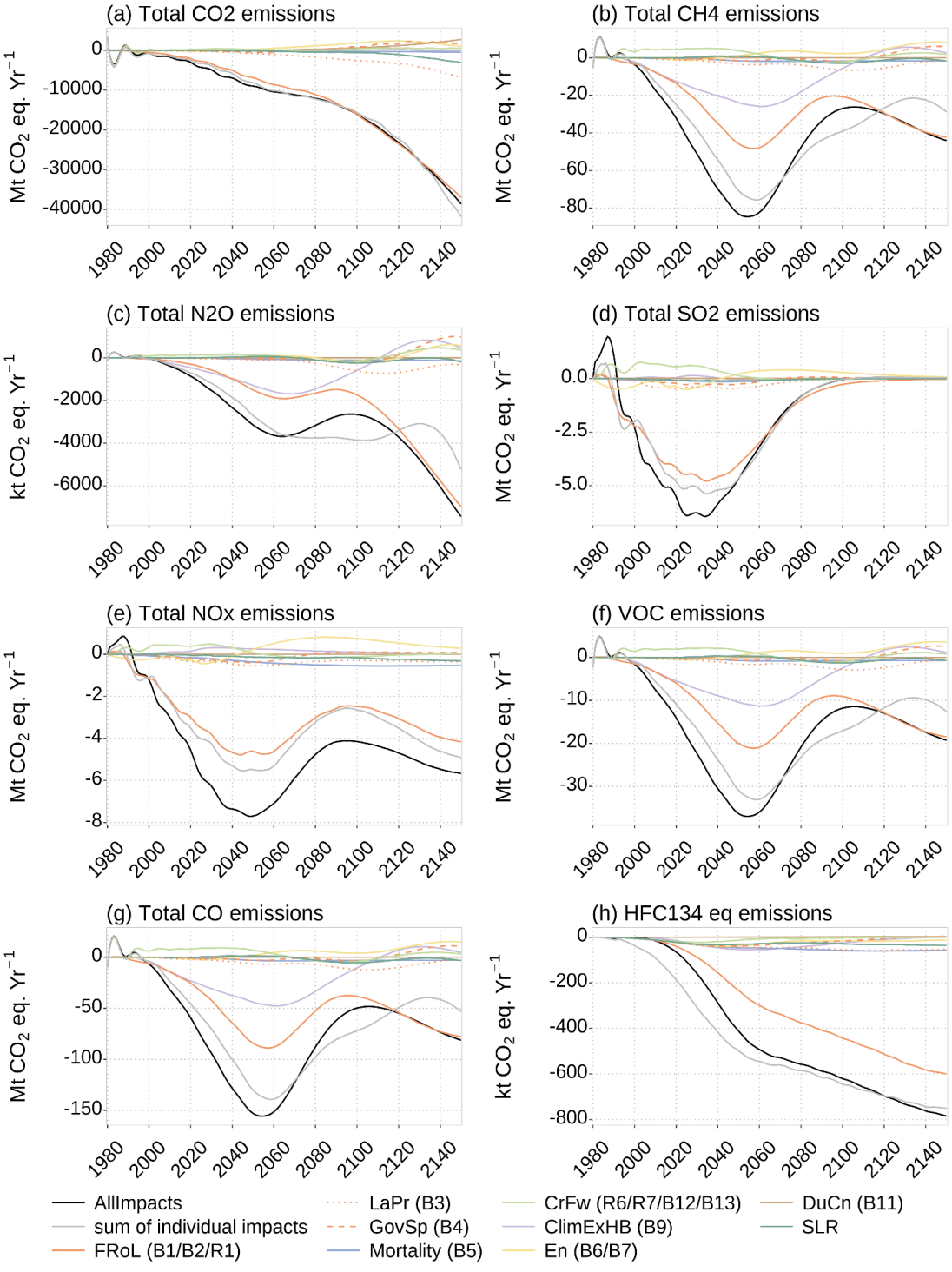

672

https://doi.org/10.5194/egusphere-2026-3072
Preprint. Discussion started: 1 July 2026

Figure 14: Same as Figure 13, but for multiple emission sources.

6. Discussion

This study examines the role of climate–society feedbacks within a coupled human–Earth system using the FRIDA v2.1, an IAM designed to explicitly represent the bidirectional feedbacks between climate and socio-economic sectors at the global level, at the expense of process complexity and regional detail. Incorporating these feedbacks is critical because climate change not only results from socio-economic processes but also actively reshapes them, creating dynamic, two-way interactions that influence emissions trajectories and system resilience. These feedbacks are only weakly represented in many conventional IAMs, potentially leading to incomplete representations of future climate risks.

FRIDA integrates several impact channels that link climate dynamics to six societal modules—Energy, Finance, Demography, Human Behaviour, Land Use, and Resource Infrastructure—and feeds resulting changes back into the climate system through altered greenhouse gas emissions (Schoenberg et al., 2025a). We organise the FRIDA impact channels (Wells et al., 2026) into nine broader categories: economic impacts, disaggregated into three channels linking climate change to (i) loan failure rates, (ii) labour productivity, and (iii) government expenditure; (iv) energy system impacts on infrastructure, demand, and supply; (v) demographic impacts; (vi) impacts on resources and concrete infrastructure; (vii) behavioural responses to climate extremes; (viii) impacts on crop productivity and freshwater availability; and (ix) financial risks associated with sea-level rise. Together, this framework enables a more comprehensive representation of coupled climate–society dynamics.

The primary and dominant mechanism in the overall system is the climate-induced loan defaults, which suppresses investments and triggers severe cascading effects that propagate throughout the global economy. Damage to bank assets reduces investment capacity and innovation, increases debt-to-GDP ratios, weakens government expenditure, and lowers labour productivity, creating reinforcing feedbacks that continually reduce global economic output. Because macroeconomic performance strongly constrains consumption and production across sectors, these economic disruptions propagate throughout the rest of the model, indirectly driving major declines in energy demand, food demand, concrete production, and crop yield. The dominance of these economic channels highlights the central role of finance and investment dynamics in shaping long-term climate–society trajectories within FRIDA.

Climate impacts on labour productivity, primarily associated with worker exposure to heat, and impacts on government expenditure through increased infrastructure repair costs act as secondary effects. These channels contribute to broader economic damages but remain substantially less influential than the cascading financial impacts associated with loan defaults. In contrast, the direct impacts on mortality, behavioural adaptation in dietary norms, concrete durability, and land

https://doi.org/10.5194/egusphere-2026-3072
Preprint. Discussion started: 1 July 2026

use are classified as marginal from a system-wide perspective, since they produce important sector-specific responses but exert comparatively limited influence on the full system when acting individually.

Although FRIDA incorporates many climate impacts across society, the results indicate that the dominant pathways are ultimately economic. This is broadly consistent with the canonical insight introduced by William Nordhaus that climate damages should be integrated into macroeconomic analysis. However, FRIDA differs substantially from conventional DICE-type frameworks in both qualitative and quantitative terms. Whereas DICE primarily represents climate damages as reductions in the level of economic output, FRIDA exhibits growth-type damages in which impacts propagate through investment, productivity, and innovation processes, generating persistent reductions in economic growth rates. Consequently, FRIDA produces substantially larger economic damages per degree of warming, reflecting the cumulative and cascading effects of climate-induced loan defaults and cross-sector interactions. These findings suggest that financial-sector vulnerabilities may constitute a key amplification mechanism through which climate impacts propagate across coupled human–Earth systems. Future work should therefore further investigate the representation of banking, credit, investment behaviour, sovereign debt dynamics, and financial adaptation within IAM frameworks, as well as additional feedbacks and nonlinearities emerging from interactions between financial systems and the real economy under climate stress.

Our results further highlight that climate–society interactions are inherently nonlinear, with system responses emerging from interactions among climate channels through shared state variables, structural constraints, and dynamic feedback processes. Importantly, the strength of nonlinear interactions is not necessarily determined by the magnitude of individual impact channels; even relatively small channels can contribute substantially when they influence shared constraints or interact strongly with other processes. This is illustrated by an additional targeted experiment in which the coupled simulation excludes the *FRoL* impact channel yet still produces nonlinear responses in food demand and crop yield comparable in magnitude to those in the *AllImpacts* case (Figure B1). This suggests that nonlinear system behaviour is governed less by the size of an individual impact channel than by the extent to which multiple channels interact through common endogenous variables and structural constraints. Food demand exhibits the strongest nonlinearity in the model due to a regime-switching mechanism between norm-driven and accessibility-constrained demand. Agricultural water withdrawal displays the second strongest nonlinearity, arising from multiplicative coupling between per-hectare water requirements, irrigated area, and cropland extent, all of which depend on shared limitations in land and water availability. Crop yield exhibits intermediate nonlinear behaviour because it co-evolves with irrigation, land allocation, and economic inputs such as fertilizer use, thereby inheriting nonlinear dynamics from both economic and biophysical systems. The surface temperature anomaly also exhibits pronounced nonlinear behaviour, driven by heterogeneous emissions pathways, nonlinear carbon-cycle dynamics and inertia of ocean–atmosphere heat exchange.

https://doi.org/10.5194/egusphere-2026-3072
Preprint. Discussion started: 1 July 2026

An important implication of these results is that aggregate indicators can conceal substantial underlying nonlinearities. This is particularly evident in total greenhouse gas emissions and aggregate energy demand, where opposing or heterogeneous component responses can produce apparently smooth aggregate trajectories despite strong nonlinear dynamics within individual sectors. As a result, focusing only on aggregate outcomes may obscure critical cross-sectoral interactions and vulnerabilities. Overall, our findings support a growing body of literature (e.g. Yokohata et al., 2019; Zscheischler, 2024; Ebi, 2025) emphasizing that climate risks emerge not only from isolated sectoral damages, but also from cascading interactions and endogenous responses within coupled human–Earth systems.

Broadly, the model demonstrates that nonlinear and threshold-like dynamics can emerge even without explicitly modelled tipping elements, solely through the interaction of coupled feedback processes across sectors. Given that FRIDA v2.1 does not yet include several potentially important climate–society feedbacks, such as wildfire dynamics, disaggregated energy-demand responses, wind-related impacts, broader biodiversity interactions, stochastic climate variability, or explicit Earth-system tipping processes such as permafrost thaw—our results may represent a conservative estimate of the nonlinear behaviour that could arise in more comprehensively coupled human–Earth system models. Future developments of FRIDA will therefore investigate how the inclusion of additional feedback mechanisms, including internally represented tipping dynamics in both Earth and social systems, further alters risk propagation and long-term coupled trajectories.

7. Concluding remarks

This study demonstrates that explicitly representing climate–society feedbacks within a coupled human–Earth system can substantially alter long-term socioeconomic and climate trajectories relative to conventional IAM approaches. By integrating bidirectional interactions across economic, demographic, behavioural, land-use, energy, and resource systems, FRIDA reveals how climate impacts propagate through interconnected feedback structures rather than remaining confined to isolated sectors. The results highlight the importance of endogenous socioeconomic responses, cascading effects, and cross-sectoral interactions in shaping future climate risks.

A key implication of this work is that climate damages may emerge less as isolated losses in economic output and more as persistent disruptions to the processes that sustain economic growth, including investment, productivity, and innovation. In this context, financial-system vulnerabilities appear to play a particularly important role in amplifying and transmitting climate impacts across sectors. More broadly, the model demonstrates that strongly nonlinear and threshold-like dynamics can arise endogenously from tightly coupled feedback processes, even in the absence of explicitly represented tipping elements.

https://doi.org/10.5194/egusphere-2026-3072
Preprint. Discussion started: 1 July 2026

These findings reinforce the need for next-generation IAMs to move beyond simplified representations of climate damages toward more integrated depictions of coupled climate–society dynamics. While FRIDA v2.1 remains limited by its global aggregation and incomplete representation of several potentially important feedbacks, the framework provides a basis for systematically exploring cascading risks, cross-sectoral vulnerabilities, and nonlinear responses within coupled human–Earth systems. Future developments incorporating additional climate, ecological, and socioeconomic feedbacks will be essential for improving the assessment of long-term climate risks and the effectiveness of mitigation and adaptation strategies under real-world conditions.

Appendix A

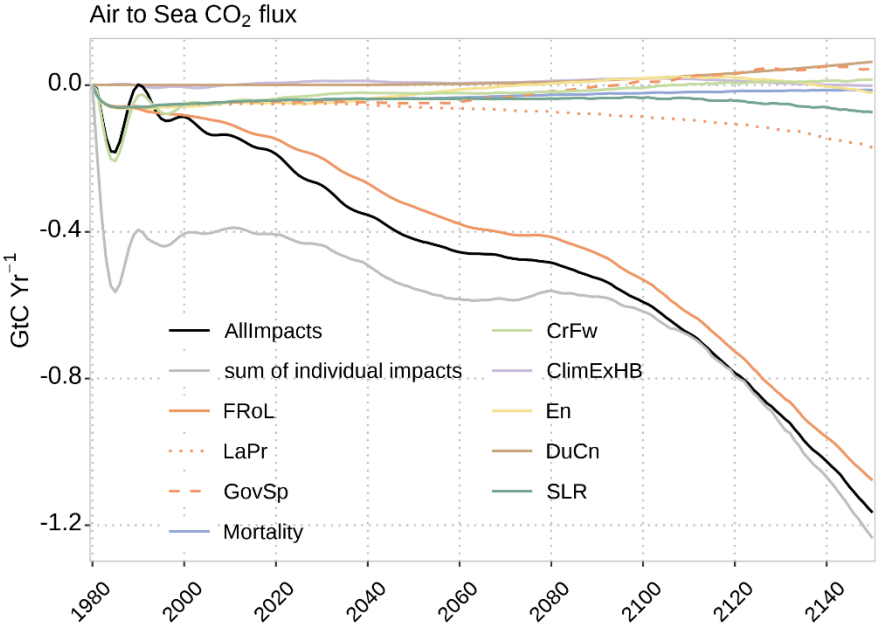

Figure A1: Effects of the climate impacts shown as deviations from the *NoImpacts* in absolute values, for Air-Sea CO_2 flux. The *AllImpacts* projection is shown as the solid black line, while individual climate impact channels are shown as coloured lines. Impact channels on labour productivity (*LaPr*) and Government expenditure (*GovSp*) are indicated by the same colour as that of *FRoL*, but in dotted and dashed lines respectively, to imply that these are part of the economic module. The solid grey lines represent the sum of the individual impacts. All the lines are median representatives of the 100,000-large ensemble.

https://doi.org/10.5194/egusphere-2026-3072
Preprint. Discussion started: 1 July 2026

Appendix B

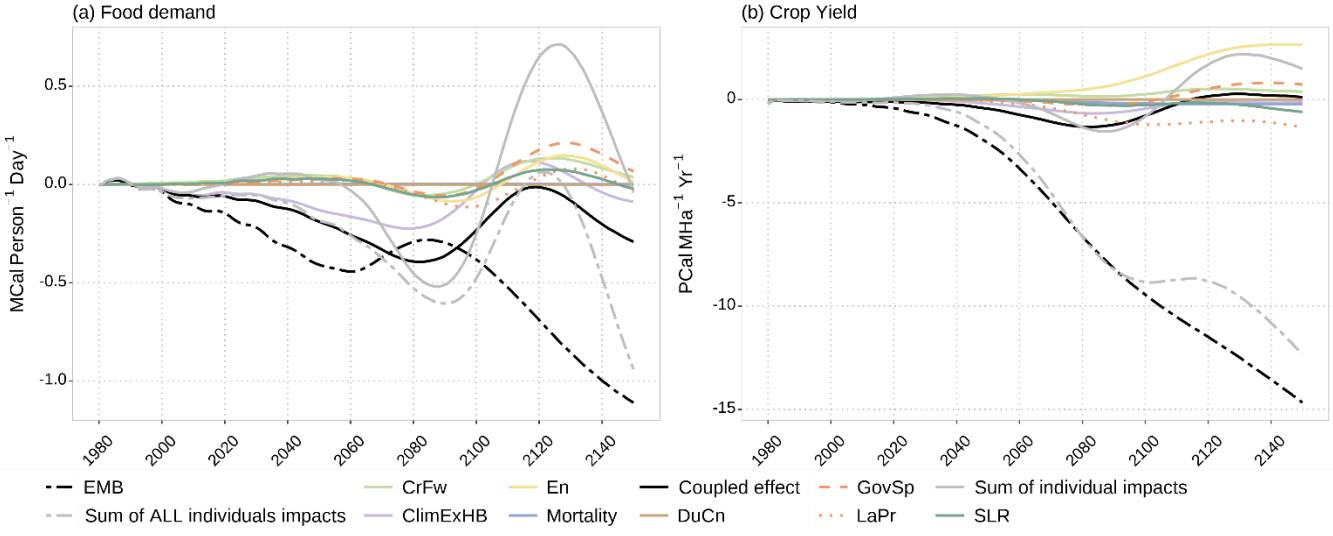

Figure B1: Results from the targeted experiment (all impact channels without the FRoL), for (a) Food demand and (b) crop yield, indicating that the nonlinearities exist even in the absence of the dominant impact channel. All the values are absolute deviations from the *NoImpacts*. The *AllImpacts* projection is shown as the solid black line, while individual climate impact channels are shown as coloured lines. Impact channels on labour productivity (LaPr) and Government expenditure (GovSp) are indicated by the same colour as that of FRoL, but in dotted and dashed lines respectively, to imply that these are part of the economic module. The solid grey lines represent the sum of the individual impacts from the targeted experiment. Solid black lines are the coupled effect of all the impact channels in the targeted experiment. Broken grey and black lines indicate the sum of ALL the impact channels (including *FRoL*) and the couped effect in the *AllImpacts* case respectively. All the lines are median representatives of the 100,000-large ensemble.

Code and data availability

The codes and data used to prepare the plots in this paper are available at https://doi.org/10.5281/zenodo.20417833 (Adakudlu, 2026). Version 2.1 of the full FRIDA model can be found at https://doi.org/10.5281/zenodo.15310860 (Schoenberg et al., 2025b). The full infrastructure to run scenario ensembles with FRIDA is hosted on GitHub https://github.com/BenjaminBlanz/WorldTransFrida-Uncertainty.

Author contributions

Conceptualization: AM, CM. Experimental design: AM. Writing – original draft: AM, CM. Writing – review and editing: all authors. Investigation: AM, CM, CW, WS, BB, LR, BC, JR, CS. Methodology: AM, WS, CW, BB, LR, BC, JR, ANL. Software: WS, BB. Visualization: AM. Funding acquisition: WS, CM, CS.

https://doi.org/10.5194/egusphere-2026-3072
Preprint. Discussion started: 1 July 2026

Competing interests

The authors declare that they have no conflict of interests.

Disclaimer

Copernicus Publications remains neutral with regard to jurisdictional claims made in the text, published maps, institutional affiliations, or any other geographical representation in this paper. While Copernicus Publications makes every effort to include appropriate place names, the final responsibility lies with the authors. Views expressed in the text are those of the authors and do not necessarily reflect the views of the publisher.

Acknowledgements

The authors would like to thank the WorldTrans consortium for the discussions and feedbacks during meetings. The authors acknowledge the computing resources provided by the Deutsches Klimarechenzentrum (DKRZ), allocated by its Scientific Steering Committee under project IDs 0033 and 1275, that were used to run the uncertainty ensembles for this paper.

Financial support

This research was supported by the Horizon Europe research and innovation programs under grant agreement no. 101081661 (WorldTrans – Transparent Assessments for Real People).

References

Adakudlu, M.: Codes and data for producing the figures in Adakudlu et al (2026) [Dataset], Zenodo, https://doi.org/10.5281/zenodo.20417833, 2026

Alhadeff, A. C.: Numb to the world: Degradation desensitization and environmentally responsible behaviour, Tropical Resources, 34, pp. 36–51, 2015.

Auffhammer, M., Baylis, P., Hausman, CH.: Climate change is projected to have severe impacts on the frequency and intensity of peak electricity demand across the United States, Proceedings of the National Academy of Sciences, 114(8), 1886-1891, doi:10.1073/pnas.1613193114, 2017.

Bamberg, S., Möser, G.: Twenty years after Hines, Hungerford, and Tomera: A new meta-analysis of psycho-social determinants of pro-environmental behaviour, Journal of Environmental Psychology, 27(1), 14-25, doi:10.1016/j.jenvp.2006.12.002, 2006.

https://doi.org/10.5194/egusphere-2026-3072
Preprint. Discussion started: 1 July 2026

822 Battiston, S., Mandel, A., Monasterolo, I., Schuetze, F., & Visentin, G.: A Climate Stress-Test of the Financial System,
823 Nature Climate Change, 7(4), 283–288, doi: 10.1038/nclimate3255, 2017.
824 Bolton, P., and Kacperczyk, M.: Do investors care about carbon risk?, National Bureau of Economic Research Working
825 Paper No. 26968. https://doi.org/10.3386/w26968, 2020.
826 Bonen, A., Semmler, W., & Klasen, S.: Economic Damages from Climate Change: A Review of Modeling Approaches,"
827 SCEPA working paper series. 2014-3, Schwartz Center for Economic Policy Analysis (SCEPA), The New School, 2014.
828 Bressler, R., D.: The mortality cost of carbon, Nature Communications, 12, 4467.
829 https://doi.org/10.1038/s41467-021-24487-w, 2021.
830 Burke, M., Hsiang, S. M., & Miguel, E.: Global non-linear effect of temperature on economic production. Nature, 527
831 (7577), 235–239. https://doi.org/10.1038/nature15725 , 2015
832 Carleton, T. A., Jina, A., Delgado, M. T., Greenstone, M., Houser, T., Hsiang, S., Hultgren, A., Kopp, R. E., McCusker, K.
833 E., Nath, I., Rising, J., Rode, A., Seo, H. K., Viaene, A., Yuan, J., & Zhang, A. T.: Valuing the global mortality consequences
834 of climate change accounting for adaptation costs and benefits, Quarterly Journal of Economics, 137(4), 2037–2105,
835 https://doi.org/10.1093/qje/qjac020, 2022.
836 Cialdini, R. B.: Descriptive social norms as underappreciated sources of social control. Psychometrika, 72(2), 263-268,
837 doi:10.1007/s11336-006-1560-6, 2007.
838 Cialdini, R. B., Kallgren, C. A., Reno, R. R.: A Focus Theory of Normative Conduct: A theoretical refinement and
839 re-evaluation of the role of norms in human behaviour, Advances in Experimental Social Psychology, 201-234.
840 doi:10.1016/s0065-2601(08)60330-5, 1991
841 Chen, K., De Schrijver, E., Sivaraj, S., Sera, F., Scovronick, N., Jiang, L., Royé, D., Lavigne, E., Kyselý, J., Urban, A.,
842 Schneider, A., Huber, V., Madureira, J., Mistry, M. N., Cvijanovic, I., Gasparrini, A., Vicedo-Cabrera, A. M., and MCC
843 Collaborative Research Network: Impact of population aging on future temperature-related mortality at different global
844 warming levels, Nature Communications, 15(1), 1796, doi:10.1038/s41467-024-45901-z, 2024.
845 Cromar, K. R., Anenberg, S. C., Balmes, J. R., Fann, N., Kim, S.-Y., Odell, K., Szpiro, A., and coauthors: A Global Health
846 Impacts for Economic Models of Climate Change: A Systematic Review and Meta-Analysis, Annals of the American
847 Thoracic Society,19(7), 1203-1212, doi:10.1513/annalsats.202110-1193oc, 2022.
848 Deaton, A.: Health, inequality, and economic development. Journal of Economic Literature, 41(1), 113–158,
849 https://doi.org/10.1257/002205103321544710, 2003
850 Dell'ariccia, G., Marquez, R.: Lending booms and lending standards, The Journal of Finance, 61(5), 2511-2546,
851 doi:10.1111/j.1540-6261.2006.01065.x, 2006
852 Deroubaix, A., Labuhn, I., Camredon, M., Gaubert, B., Monerie, P.-A., Popp, M., Ramarohetra, J., Ruprich-Robert, Y.,
853 Silvers, L. G., and Siour, G.: Large uncertainties in trends of energy demand for heating and cooling under climate change,
854 Nature Communications, 12(1), 5197, doi:10.1038/s41467-021-25504-8, 2021

https://doi.org/10.5194/egusphere-2026-3072
Preprint. Discussion started: 1 July 2026

Deetman, S., Marinova, S., van der Voet, E., van Vuuren, D. P., Edelenbosch, O., & Heijungs, R.:. Modelling global material stocks and flows for residential and service sector buildings towards 2050, Journal of Cleaner Production, 245, 118658, https://doi.org/10.1016/j.jclepro.2019.118658, 2020

Dietz, S., Rising, J., Stoerk, T., and Wagner, G.: Economic impacts of tipping points in the climate system, Proceedings of the National Academy of Sciences, 2021, 118(34), e2103081118, https://doi.org/10.1073/pnas.2103081118, 2021

Diaz, D., Moore, F.: Quantifying the economic risks of climate change, Nature Climate Change, 2017, 7(11), 774-782. doi:10.1038/nclimate3411, 2017

Fiddaman, T. S.: Feedback complexity in integrated climate-economy models (Ph.D. thesis). Massachusetts Institute of Technology, Sloan School of Management, Cambridge, MA, USA, 1997

Fishman, M. J., Parker, J. A., Straub, L.: A dynamic theory of lending standards, Review of Financial Studies, 37(8), 2355-2402. doi:10.1093/rfs/hhae010, 2024

Franke, J. A., Müller, C., Elliott, J., Ruane, A. C., Jägermeyr, J., Snyder, A., Dury, M., Falloon, P. D., Folberth, C., François, L., Hank, T., Izaurralde, R. C., Jacquemin, I., Jones, C., Li, M., Liu, W., Olin, S., Phillips, M., Pugh, T. A. M., Reddy, A., Williams, K., Wang, Z., Zabel, F., & Moyer, E. J: The GGCMI Phase 2 emulators: Global gridded crop model responses to changes in CO_2, temperature, water, and nitrogen (version 1.0), Geoscientific Model Development, 13, 3995–4018. https://doi.org/10.5194/gmd-13-3995-2020, 2020

Frieler, K., Volkholz, J., Lange, S., Schewe, J., Mengel, M., Rivas López, M. R., Otto, C., Reyer, C. P. O., Karger, D. N., Malle, J. T., and coauthors: Scenario setup and forcing data for impact model evaluation and impact attribution within the third round of the Inter-Sectoral Model Intercomparison Project (ISIMIP3a), Geoscientific Model Development, 17, 1–51, https://doi.org/10.5194/gmd-17-1-2024, 2024

Ford, A:. Modeling the Environment: An Introduction to System Dynamics Models of Environmental Systems, Island Press, Washington, DC, 1999

Gernaat, D. E. H. J., De Boer, H. S., Daioglou, V., Yalew, S. G., Müller, C., Van Vuuren, D. P.: Climate change impacts on renewable energy supply, Nature Climate Change, 11(2), 119-125, doi:10.1038/s41558-020-00949-9, 2021

Grimeland, M. B., Blanz, B., Schoenberg, W., and Callegari, B.: Schumpeterian disaggregation and integrated assessment: An endogenous, stock-flow consistent economy in disequilibrium for FRIDA v2.1, EGUsphere [preprint]. https://doi.org/10.5194/egusphere-2025-6342, 2026

Godfray, H. C. J., Aveyard, P., Garnett, T., and coauthors:. Meat consumption, health, and the environment, Science. 361 (6399), doi:10.1126/science.aam5324, 2018

Hope, C., Anderson, J., Wenman, P.: Policy analysis of the greenhouse effect. Energy Policy, 1993, 21(3), 327-338. doi:10.1016/0301-4215(93)90253-c, 1993

Howard, P. H., and Sterner, T.: Few and Not So Far Between: A Meta-analysis of climate damage estimates, Environmental and Resource Economics, 68(1), 197–225, https://doi.org/10.1007/s10640-017-0166-z, 2017

https://doi.org/10.5194/egusphere-2026-3072
Preprint. Discussion started: 1 July 2026

888 Intergovernmental Panel on Climate Change, Climate Change 2022: Impacts, Adaptation and Vulnerability. Contribution of
889 Working Group II to the Sixth Assessment Report of the IPCC, Cambridge University Press.
890 https://doi.org/10.1017/9781009325844, 2022
891 Kennard, H., Oreszczyn, T., Mistry, M., Hamilton, I.: Population-weighted degree-days: The global shift between heating
892 and cooling, Energy and Buildings, 271, 112315, doi:10.1016/j.enbuild.2022.112315, 2022
893 Kirk, D.: Demographic Transition Theory, Population Studies, 50, 361–387, 10.1080/0032472031000149536, 1996
894 Lesthaeghe, R.: The Unfolding Story of the Second Demographic Transition, Population and Development Rev, 36,
895 211–251, doi:10.1111/j.1728-4457.2010.00328.x, 2010
896 Lown, C., and Morgan, D, P.: The Credit Cycle and the Business Cycle: New Findings Using the Loan Officer Opinion
897 Survey, Journal of Money, Credit and Banking, Blackwell Publishing, vol. 38(6), pages 1575-1597, 2006
898 Marquez-Ramos, L., and Mourelle, E.: Education and economic growth: An empirical analysis of nonlinearities, Applied
899 Economic Analysis, 27 (79), 21–45, 2019
900 Meadows, D., H.: Thinking in systems: A primer, Chelsea Green Publishing, White River Junction, VT, 2008
901 Milford, A. B., Mouël, C. L., Bodirsky, B. L., Rolinski S. Drivers of meat consumption, Appetite, 141,
902 doi:10.1016/j.appet.2019.06.005, 2019
903 Moss, R. H., Edmonds, J. A., Hibbard, K. A., Manning, M. R., Rose, S. K., van Vuuren, D. P., Carter, T. R., Emori, S.,
904 Kainuma, M., Kram, T., Meehl, G. A., Mitchell, J. F. B., Nakicenovic, N., Riahi, K., Smith, S. J., Stouffer, R. J., Thomson,
905 A. M., Weyant, J. P., & Wilbanks, T. J.: The next generation of scenarios for climate change research and assessment, Nature,
906 463, 747–756, https://doi.org/10.1038/nature08823, 2010
907 Müller, C., Jägermeyr, J., Franke, J. A., and coauthors: Substantial differences in crop yield sensitivities between models call
908 for Functionality-Based model evaluation, Earth's Future, 12(3), doi:10.1029/2023ef003773, 2024
909 Nordhaus, W., D.: An optimal transition path for controlling greenhouse gases, Science, 258(5086), 1315-1319.
910 doi:10.1126/science.258.5086.1315, 1992
911 Nordhaus, W., D.: Revisiting the social cost of carbon, Proceedings of the National Academy of Sciences, 114(7),
912 1518–1523, https://doi.org/10.1073/pnas.1609244114, 2017
913 Nordhaus, W, D.: Evolution of modeling of the economics of global warming: Changes in the DICE model, 1992–2017,
914 Climatic Change, 148(4), 623–640, https://doi.org/10.1007/s10584-018-2218-y, 2018
915 O'Neill, B. C., Kriegler, E., Riahi, K., Ebi, K. L., Hallegatte, S., Carter, T. R., Mathur, R., and van Vuuren, D. P.: A new
916 scenario framework for climate change research: the concept of shared socioeconomic pathways, Climatic Change, 122,
917 387–400. https://doi.org/10.1007/s10584-013-0905-2, 2014
918 Ostberg, S., Schewe, J., Childers, K., Frieler, K.: Changes in crop yields and their variability at different levels of global
919 warming, Earth System Dynamics, 9(2), 479-496, doi:10.5194/esd-9-479-2018, 2018
920 Preston, S. H.: The Changing Relation between Mortality and level of Economic Development. Population Studies, 29(2),
921 231–248, https://doi.org/10.1080/00324728.1975.10410201, 1975

https://doi.org/10.5194/egusphere-2026-3072
Preprint. Discussion started: 1 July 2026

Proto, E., and Rustichini, A.: A reassessment of the relationship between GDP and life satisfaction, PLoS ONE, 8(11), e79358, 2013

Rajah, J. K., Blanz, B., Kopainsky, B., and Schoenberg, W.: An endogenous modelling framework of dietary behavioural change in the fully coupled human-climate FRIDA v2.1 model, Geoscientific Model Development, 18(18), 5997-6022. doi:10.5194/gmd-18-5997-2025, 2025

Ramme, L., Blanz, B., Wells, C., Wong, T. E., Schoenberg, W., Smith, C., and Li, C.: Feedback-based sea level rise impact modelling for integrated assessment models with FRISIAv1.0, Geosci. Model Dev., 18, 10017–10052, https://doi.org/10.5194/gmd-18-10017-2025, 2025.

Reilly, J., Paltsev, S., Strzepek, K., Webster, M., and Cai, Y.: The MIT Emissions Prediction and Policy Analysis (EPPA) Model: Description and applications, MIT Joint Program on the Science and Policy of Global Change, Report 125, 2007

Rial, J. A., Pielke, R. A., Beniston, M., and coauthors: Nonlinearities, Feedbacks and Critical Thresholds within the Earth's Climate System, Climatic Change, 65(1-2), 11-38, doi:10.1023/b:clim.0000037493.89489.3f, 2004

Riahi, K., van Vuuren, D. P., Kriegler, E., Edmonds, J., O'Neill, B. C., Fujimori, S., Bauer, N., Calvin, K., Dellink, R., Fricko, O., Lutz, W., Popp, A., Cuaresma, J. C., KC, S., Leimbach, M., Jiang, L., Kram, T., Rao, S., Emmerling, J., Tavoni, M.: The Shared Socioeconomic Pathways and their energy, land use, and greenhouse gas emissions implications: An overview, Global Environmental Change, 42, 153–168, https://doi.org/10.1016/j.gloenvcha.2016.05.009, 2017

Rodano, G., Serrano-Velarde, N., Tarantino, E.: Lending Standards over the Credit Cycle, Review of Financial Studies, 31(8), 2943-2982, doi:10.1093/rfs/hhy023, 2018

Roncoroni, A., Battiston, S., Hallegatte, S., & Rohner, D.: Climate risk and financial stability in the network of banks and investment funds, Nature Climate Change, 11, 205–211. https://doi.org/10.1038/s41558-020-00959-3, 2021

Rosenzweig, C., Elliott, J., Deryng, D., Ruane, A. C., Müller, C., Arneth, A., Boote, K. J., Folberth, C., Glotter, M., Khabarov, N., Neumann, K., Piontek, F., Pugh, T. A. M., Schmid, E., Stehfest, E., Yang, H., & Jones, J. W. : Assessing agricultural risks of climate change in the 21st century in a global gridded crop model intercomparison, Proceedings of the National Academy of Sciences, 111(9), 3268–3273, https://doi.org/10.1073/pnas.1222463110, 2014

Schoenberg, W., Blanz, B., Rajah, J. K., Callegari, B., Wells, C., Breier, J., Grimeland, M. B., Lindqvist, A. N., Ramme, L., Smith, C., Li, C., Mashhadi, S., Muralidhar, A., and Mauritzen, C.: An overview of FRIDA v2.1: a feedback-based, fully coupled, global integrated assessment model of climate and humans, Geosci. Model Dev., 18, 8047–8069, https://doi.org/10.5194/gmd-18-8047-2025, 2025a.

Schoenberg, W., Blanz, B., Ramme, L., Wells, C., Grimeland, M., Callegari, B., Breier, J., Rajah, J., Nicolaidis Lindqvist, A., Mashhadi, S., Muralidhar, A., and Eriksson, A.: FRIDA: Feedback-based knowledge Repository for IntegrateD Assessments (v2.1), Zenodo [code], https://doi.org/10.5281/zenodo.15310860, 2025b.

Schoenberg, W., and Callegari, B.: The role of persistent climate-driven financial effects in estimating climate damages through Integrated Assessment Models, submitted, 2026

https://doi.org/10.5194/egusphere-2026-3072
Preprint. Discussion started: 1 July 2026

Schumpeter, J. A.: The theory of economic development; an inquiry into profits, capital, credit, interest, and the business cycle, Harvard University Press, Cambridge, 930 Mass., 1934.

Schwanitz, V. J., Piontek, F., Bertram, C., & Luderer, G.: Long-term economic consequences of climate change: The importance of damage functions, Environmental and Resource Economics, 73, 1–26. https://doi.org/10.1007/s10640-018-0274-5, 2019

Sparkman, G., Walton, G. M.: Dynamic norms promote sustainable behaviour, even if it is counternormative. Psychological Science, 28(11), 1663-1674, doi:10.1177/0956797617719950, 2017

Stern, N.: The structure of economic modeling of the potential impacts of climate change: Grafting gross underestimation of risk onto already narrow science models, Journal of Economic Literature, 51(3), 838–859. https://doi.org/10.1257/jel.51.3.838, 2013

Tol, R. S. J.: The double trade-off between adaptation and mitigation for sea level rise: an application of FUND, 2007, Mitig.Adapt. Strateg. Glob. Chang., 12, 741–753, 2007

Tol, R. S. J.: The economic impacts of climate change, Review of Environmental Economics and Policy, 12(1), 4–25. https://doi.org/10.1093/reep/rex027, 2018

Van Vliet, M. T. H., Wiberg, D., Leduc, S., Riahi, K.: Power-generation system vulnerability and adaptation to changes in climate and water resources, Nature Climate Change, 6(4), 375-380, doi:10.1038/nclimate2903, 2016

Van Valkengoed, A. M., Perlaviciute, G., and Steg, L.: Representing the drivers of lifestyle change in Integrated Assessment Models using theories from environmental psychology: introducing the Motivation, Agency, and Past Behaviour (MAP) framework. Environmental Research Communications, 7(3), 032001, doi:10.1088/2515-7620/adb9bf, 2025

Wells, C., Blanz, B., Ramme, L., and coauthors: The Representation of Climate Impacts in the FRIDAv2.1 Integrated Assessment Model. Geoscientific Model Development. (Preprint). doi:10.5194/egusphere-2025-2756, 2025

Wells, C. D., Ramme, L., Smith, C., Breier, J., Muralidhar, A., Li, C., Gjermundsen, A., Schoenberg, W. A., Blanz, B., and Mauritzen, C.: FRIDA-Clim v1.0.1: a simple climate model with process-based carbon cycle used in the integrated assessment model FRIDAv2.1, Geosci. Model Dev., 19, 1429–1453, https://doi.org/10.5194/gmd-19-1429-2026, 2026

World Bank: Bank nonperforming loans to total gross loans (%), 2023.

Yokohata, T., Tanaka, K., Nishina, K., Takahashi, K., Emori, S., Kiguchi, M., Iseri, Y., Honda, Y., Okada, M., Masaki, Y., Yamamoto, A., Shigemitsu, M., Yoshimori, M., Sueyoshi, T., Iwase, K., Hanasaki, N., Ito, A., Sakurai, G., Iizumi, T., Oki, T.: Visualizing the interconnections among climate risks. Earth S Future, 7(2), 85–100. https://doi.org/10.1029/2018ef000945, 2019